2017

A Coupling Analysis Approach to Capture Unexpected Behaviors in Ares 1

David Kis
Iowa State University

A coupling analysis approach to capture unexpected behaviors in Ares 1

by

David Kis

A thesis submitted to the graduate faculty

in partial fulfillment of the requirements for the degree of

MASTER OF SCIENCE

Major: Aerospace Engineering

Program of Study Committee:
Christina Bloebaum, Major Professor
Ran Dai
Peng Wei
David Sly

Iowa State University

Ames, Iowa

2017

TABLE OF CONTENTS

LIST OF FIGURES

LIST OF TABLES

NOMENCLATURE

LSCES	Large Scale Complex Engineered Systems
MDO	Multidisciplinary Design Optimization
NASA	National Aeronautics and Space Administration
T/O	Thrust Oscillation
SRM	Solid Rocket Motor
VDD	Value Driven Design
ICD	Interface Control Documentation
DSM	Design Structure Matrix
RANS	Reynolds-Averaged Numerical Solution
RSRM	Reusable Solid Rocket Motor
CFD	Computational Fluid Dynamics
VS	Vortex Shedding Frequency
MCA	Multidisciplinary Coupling Analysis
ISS	International Space Station

ACKNOWLEDGMENTS

I would like to start off by expressing my sincerest gratitude to my major professor and advisor, Dr. Christina Bloebaum. Her support and guidance through my Masters of Science degree has helped push me academically to endure and succeed through this challenging program. I would also like to thank all of my friends, lab mates, and mentors of the MODEL lab Garima, Subu, Ben, Rao, Naz, Akash, Suresh, Matt, Syed, and Robert. The love and support of everyone in this lab has made my graduate studies an experience I will never forget.

In addition, I would like to acknowledge my good friend and research partner Chris Wenger, whose support, teamwork and drive has helped me immensely through my studies and journey here at Iowa State. I would also like to thank my good friends Eric and Tor whose humor and friendship has helped made my stay here at Iowa State an amazing one.

Lastly, I would like to thank my parents and my brothers whose unconditional love and support has helped guide me through the difficulties I faced while working on my degree.

ABSTRACT

Coupling of physics in large-scale complex engineering systems must be correctly accounted for during the systems engineering process. Preliminary corrections ensure no unanticipated behaviors arise during operation. Structural vibration of large segmented solid rocket motors, known as thrust oscillation, is a well-documented problem that can effect solid rocket motors in adverse ways. Within the Ares 1 rocket, unexpected vibrations deemed potentially harmful to future crew were recorded during late stage flight that propagated from the engine chamber to the Orion crew module. This research proposes the use of a coupling strength analysis during the design and development phase to identify potential unanticipated behaviors such as thrust oscillation. Once these behaviors and couplings are identified then a value function, based on research in Value Driven Design, is proposed to evaluate mitigation strategies and their impact on system value. The results from this study showcase a strong coupling interaction from structural displacement back onto the fluid flow of the Ares 1 that was previously deemed inconsequential. These findings show that the use of a coupling strength analysis can aid engineers and managers in identifying unanticipated behaviors and then rank order their importance based on the impact they have on value.

CHAPTER 1

INTRODUCTION

Large Scale Complex Engineered Systems (LSCES) often have cases where unintended consequences or unanticipated behaviors occur during system operation. The severity of these behaviors can vary in degree, some having little impact on system performance, while others having major contributions to system failure. After the fact, fixes are made to these systems to ensure proper system performance. This adds additional time and cost to the project. The ability to identify and capturing these behaviors during the design and development phase is important to ensure system performance and prevent cost overruns. Early identification of potential problems also allows engineers to address the issues at the system level. This allows for more flexibility to the possibility of solutions, and allows the option to fix root causes of said problems instead of designing a fix for the symptoms [1]. The goal of this research is to look at an example of a LSCES in depth, perform a forensics study, and present a coupling strength approach from the field of Multidisciplinary Design Optimization (MDO) as a possible means of identifying unanticipated behaviors that may occur in LSCES. From that information a Value function will be presented to evaluate the total impact the unidentified problem might have had on mission success if it were captured.

On October 28, 2009 the National Aeronautics and Space Administration (NASA) conducted a successful test launch of the Ares-1X which was a proof of concept launch vehicle designed as part of the Constellation Program. The intended mission for the Ares 1 was to launch Orion, the crew module, into orbit for missions which spanned from completion of the International Space Station to a manned mission to Mars [2]. During the testing of Ares 1-X large vibrations and perturbations within the engine chamber were recorded during first stage flight.

These vibrations propagated from the engine chamber to the crew module, where if crew members were present, had sufficient strength to pose a hazard to crew health and ability to operate Ares 1 during ascent. An investigation ran by NASA found Thrust Oscillation (T/O) as the contributing factor to the vibrations and perturbations recorded.

Thrust Oscillation is a well-known phenomenon that occurs within the combustion chamber of a Solid Rocket Motor (SRM). It is caused by a coupling phenomenon between the propellant flow in the engine, acoustic modes of the chamber, and the structures response. During combustion, unstable flow is produced from sudden transitions in the combustion chambers such as protrusions in the flow [3]. These sudden transitions cause turbulent flow to form downstream of the protrusion which in turn generates vortex shedding. The vortices from the vortex-shedding, generated by the protrusion, travel downstream and eventually interact with the surface of the engine chamber, causing waves of pressure that excite the structure. If the vortex shedding frequencies produced correspond to the acoustic mode frequencies of the engine, pressure oscillations are generated which causes a net increase of energy inside the engine chamber and can even travel upstream to the flow [4]. The structure of the rocket then develops a structural response, where if the dampening factor is greater than the excitation energy generated by the pressure oscillations the vibrations dampen out. In the case where the pressure oscillation frequencies correspond to the resonance frequency of the structure, thrust oscillation occurs [3]. If T/O is not mitigated, the engine chamber may build up a high level of instability, affecting the remaining rocket structure, and eventually propagating up to the crew module as was the case in the Ares 1-X [2].

NASA engineers made numerous investigation approaches, and a team, named the T/O mitigation team, was developed to tackle the issues recorded on the Ares 1-X. Numerous

mitigation approaches were investigated, but ultimately 2 additions were implemented to mitigated T/O. The first addition being an upper C-spring isolator, and the second an upper stage fuel tank damper name the LOX damper [5]. The combination of these two additions served to be the final solution to dampen out the T/O event. The C-spring acted as a shock absorber by absorbing and damping some of the energy created by Trust Oscillation and was placed between the segments of the rocket. The LOX damper served to leverage the kinetic energy of the liquid oxygen in the tank to dampen out vibrations caused by the fluid flow. Both additions combined gave the T/O mitigation team a higher confidence factor in the de-tuning of Ares 1-X [5].

Typically the modeling for LSCES is done separately where designated teams are assigned subsystems to work on. In the case of the Ares 1 the fluids team and structures team communicated with interface control documentations, where only direct inputs from one subsystem to another is captured. The initial analysis during the design phase should an inconsequential feedback from structures and an iterative process to define the physics was ignored to save on computational time. However, the T/O mitigation team found after the launch that the structures response to the pressure oscillations had a greater impact on fluid flow of the engine and creating T/O than previously assumed. If a means existed to identify the importance of the couplings and feedbacks in the system physics during the design phase, dampening could occur by design, rather than by mitigation.

In this research, an investigation will be made into the T/O event of the Ares 1-X to determine if the feedback and feedforward physics associated with T/O could have been captured during the design phase. The thesis proposes a Multidisciplinary Coupling Analysis (MCA) as a way to identify critical feedbacks between subsystems and to capture the interactions subsystems have with each other, instead of using separate a analysis for each subsystem. An investigation

will be made to identify key contributors to thrust oscillation and a value model will be developed to determine the impact of eliminating these key couplings could have on cost and total mission success.

CHAPTER 2

RESEARCH QUESTIONS

The following chapter contains the research questions this thesis aims to answer and were formed by an unforeseen behavior found on the Ares 1 and its impact it had on NASA.

Research Question 1

"Can using a coupling strength analysis in Multidisciplinary Design Optimization provide a means to capture unexpected or unintended consequences during the design and development phase of Large Scale Complex Engineered Systems?"

This research question will be addressed by breaking down the physics of Thrust Oscillation into disciplines. These disciplines are defined to be teams of engineers that would specialize in their respective fields and pass along validated results to managers and other disciplines they interface with. For instance a discipline of importance in the T/O event would be fluids, where the engineers assigned to this discipline are in charge of modeling the physics associated with the fluid flow within the engine. Three major disciplines were identified: fluids, structures and acoustics. These disciplines will be used in a coupling strength analysis to identify the relative importance of each behavior variable through a comparative analysis. The methodology to capture these behavior variables and the impact they have on disciplines is explored more in depth in the background chapter of this research.

Research Question 2

"How does capturing the coupling information of the T/O event in the Ares 1 during the design phase impact the overall value of the mission?"

This research question will be addressed by developing a value function for a hypothetical mission to the International Space Station (ISS). The value function proposed will be broken down

into 2 major attributes: Probability of Mission Success and Cost. The behavior variables captured in the coupling analysis, as well as others pertaining to the mission, will be used to calculate these attributes that will be used to calculate the overall value of the design. Once developed the capturing of T/O will be eliminated and a comparative analysis of the total value will be made between capturing the coupling of T/O and eliminating it. The difference in value will give insight to the cost vs benefits of adding additional computational time to capture unexpected behaviors that can occur when designing LSCES.

Organization of Thesis

The thesis will be broken down first by stating the research questions that this research aims to answer with the proposed approach to address them. Next a detailed background of the physics associated with Thrust Oscillation will be covered as this was the major unforeseen behavior in the Ares 1, as well as the proposed methodology to identify Thrust Oscillation during the design phase. Lastly an investigation into the research questions is made in the subsequent chapters with the methodologies proposed and conclusions will be drawn from the models and tests.

CHAPTER 3

BACKGROUND

Systems Engineering

Large-Scale Complex Engineered Systems by definition are complex, multidisciplinary, and involve numerous individuals with varying expertise to design and develop. In-order to tackle the ever growing complexity of designing such systems a new field called systems engineering evolved in the 1950's. The development process of LSCES has grown in both time and cost at unsustainable rates, where in some cases these systems are too big to discontinue [6]. The current practice to develop and design these systems is a requirements-driven Systems Engineering (SE) approach where the stakeholder state's the needs and wants in the form of requirements. Requirements represent the expected behavior of the system based on customer needs, and essentially state what is not desired in the system. The primary requirements are flowed down to subsystem design engineers who build subsystems or accordance with requirements set by system's above them. This is done by developing sub-system requirements and a flowed down of requirements go down to the design level where the design engineers develop the necessary subsystems to complete the specified design requirements [7]. Once the requirements are defined are met at the lower level they are then integrated and verified and move up through the design process in a systems engineering model known as the "Vee" model represented in Figure 1 [8].

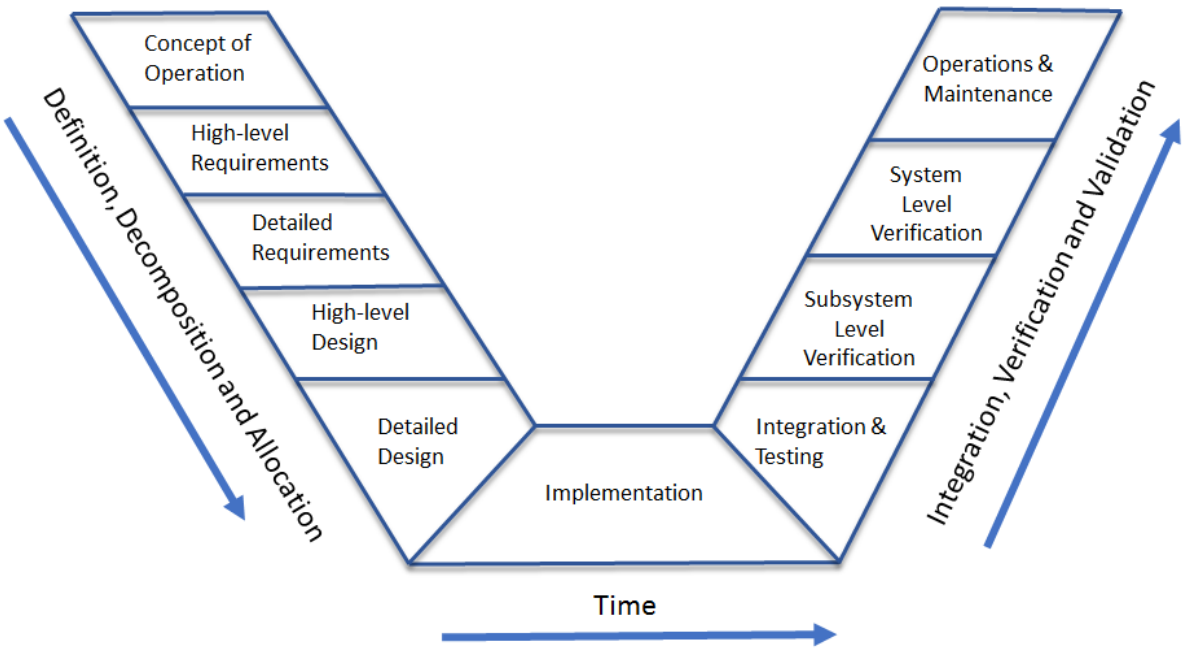

Figure 1. *Systems Engineering Vee-Model*

The requirements set by stakeholders using the "Vee-Model" act more as proxies to the true preferences of the stakeholders. To address this an economic-based design methodology called Value Driven Design (VDD) is proposed that uses value functions to capture the true preferences of stakeholders [9,10,40,49]. Value functions are mathematical representations to the true preferences of stakeholders and breakdown the design process in terms of an valued benefit, typically in the form of profit or mission success rate [44,49]. The Value Driven Design methodology and value functions discussed within this research is a way of thinking that will be used to address research question 2.

In traditional requirements-based system engineering methodologies a Interface Control Documentation (ICD) is used to address interactions between subsystems in a hierarchical decomposition [11,51,53]. A 3 level hierarchical decomposition of the Ares 1 is presented in Figure 2 below as an example. Boundaries are representative of subsystems, where these boundaries are used to define couplings such as subsystem couplings [7,51]. In LSCES the

behavior of these couplings can be highly complex, with numerous interactions occurring as the amount of subsystems grow. Capturing the highly complex couplings within a LSCES cannot be addressed through ICD's alone.

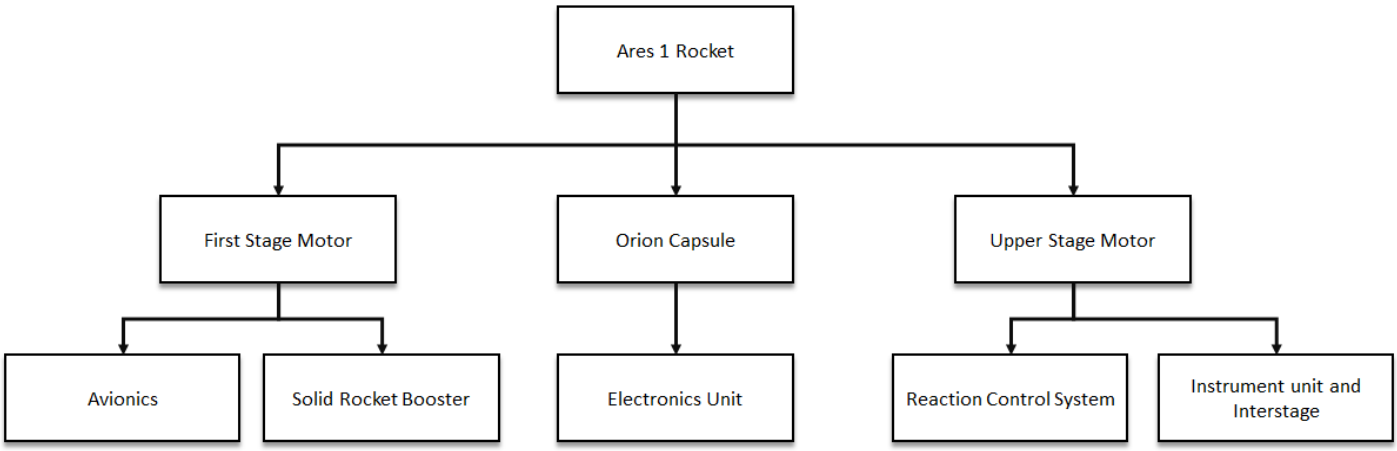

Figure 2. *Hierarchical Decomposition of the Ares 1*

Multidisciplinary Design Optimization

Multidisciplinary Design Optimization (MDO) was developed in the 1980's as a means to address the interactions between disciplines in the design of LSCES. Within MDO couplings are captured and modeled in both the analysis and optimization of a system's design [50,53]. MDO uses an optimization framework that handles a system composed of many subsystems and uses the couplings between these subsystems to ensure consistency in physics [12]. This is done with computer simulations that are used to model subsystem interactions, which enable a system analysis that is used within the larger system optimization. To better understand the process an example problem is presented.

A typical engineering problem can most easily be broken down into disciplines whose workers within have expertise in their respected fields [15]. Traditionally system designs would be broken down into a hierarchical model that is composed in an arbitrary ordering where the optimal point would be heavily influenced by sequence [13]. As it is shown in Figure 3 a below a

traditional rocket system is broken down between interacting disciplines. The design is then optimized first by the structures subsystem, then followed by the propulsion and lastly the fluids. An analysis is performed within each discipline, where design variables are varied and design optimums are searched for within each discipline. It can be seen that an "optimal" design will converge from the traditional method but the interactions between the subsystems is lost unless a full convergence is made in each subsystem every time a design variable is changed or a step taken in the optimization program. This requires an enormous amount of computational time which wouldn't be feasible in the design of a LSCES.

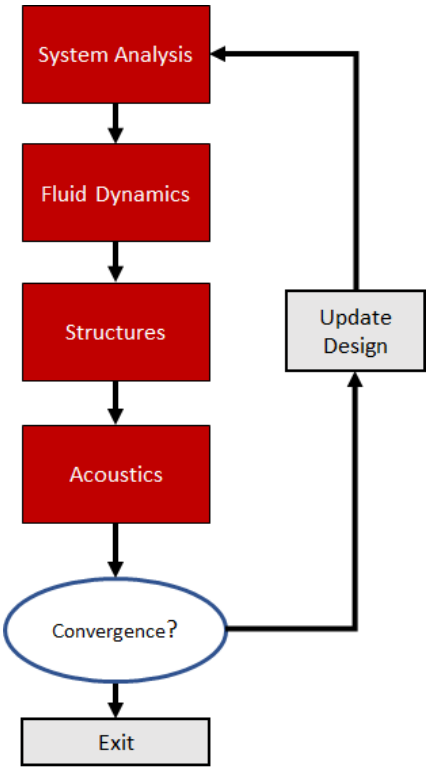

Figure 3. *Traditional Optimization Method*

In the early 1980's Jaroslaw Sobieszczanski-Sobieski developed a way to address the loss of coupling information in a hierarchical format where subsystems are separate but coupled [14]. The approach focused on preserving system couplings, which were the outputs of a subsystem analysis impacting another subsystem analysis, also known as behavior variables. By preserving

behavior variables the subsystem decomposition can be linear and a local linearized optimization problem could then be used to determine the impact of subsystems on each other. This approach can then take advantage of sequential linear optimization of the system without losing information of subsystem couplings. The MDO approach that Sobieski showcased in his paper is simplified in Figure 4 below:

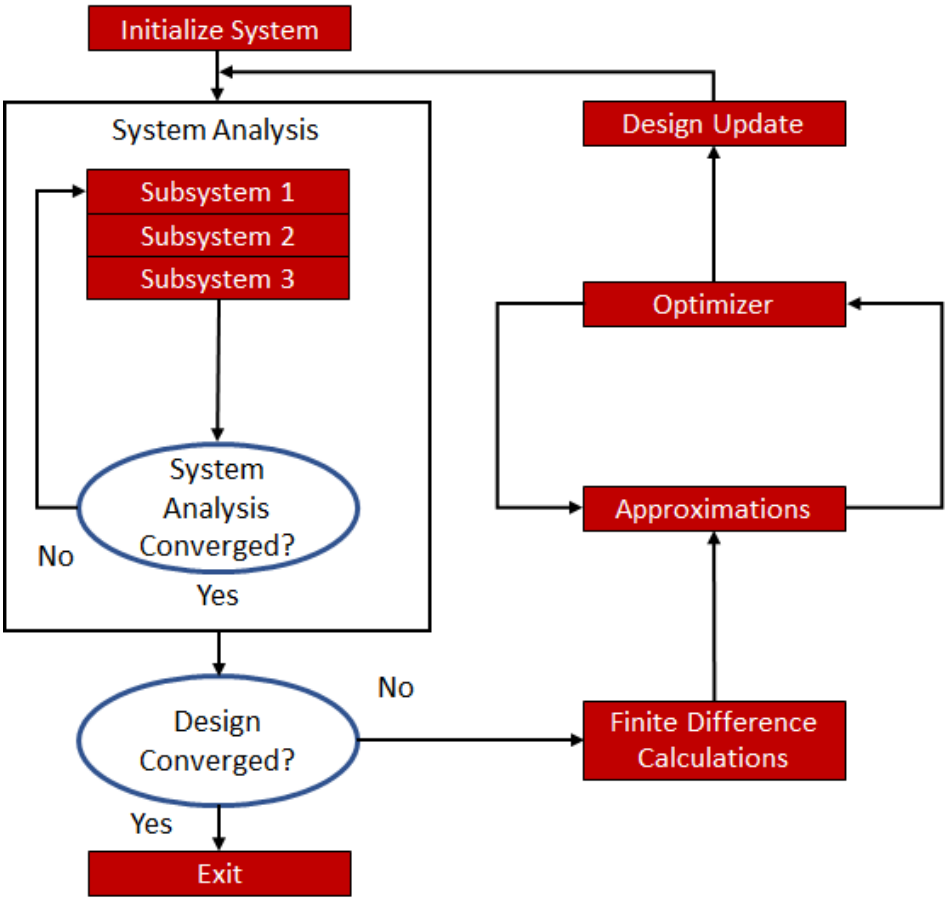

Figure 4. *MDO Flowchart*

The optimization problem works by first initializing the system, where then the information is pasted to the system analysis and broken down into its respective subsystems. The subsystem's are then converged through an iterative process, where the hierarchic sequence of subsystems matters in determining computational time till convergence. For instance in the case where subsystem feedbacks are 0, the sequence only needs to be executed once till convergence is met.

In the case where a sequence contains multiple subsystem feedbacks the required computational time till convergence goes up. The smaller system feedbacks the less time till subsystem convergence is met. Once the system analysis is converged, a finite difference calculation is used to propagate the design and behavior variables within each subsystem. A simplistic way to view this would be through the use of a Design Structure Matrix (DSM) which is mentioned in detail in the next section. Approximations for the total impact these variables have on the system are then needed to account for the subsystem interactions, which would later be used to update the design. To find the impacts the design and behavior variables have on the local subsystems Sobieski's Global Sensitivity Equations are used.

Design Structure Matrix

A simplistic way to represent subsystem interactions within a complex system is through the use of a Design Structure Matrix (DSM). DSM's showcase feed forwards and feedbacks of subsystems in a matrix, where feed forwards and feed backs are represented by connecting lines. Depending on the size of a DSM the method for showcasing the interactions can change, in the cases with many subsystems and interacting parts the matrix can more easily be represented with dots or markers representing couplings. In Figure 5 a coupled system is shown with three subsystems and its interacting parts. The X's in the figure represent the design variables which are independent variables used to define the subsystems. The Y's represent the behavior variables which are the behavior of the subsystem with respect to a particular design variable input. The behavior variables in the case shown below are coupled, meaning that the behavior variables of each subsystem impact the neighboring subsystems. In Figure 6 a DSM is created from the system shown in Figure 5. In a DSM the behavior variables are represented by dots, and the design variables are represented by arrows directly going into the subsystems. As the number of

subsystems increases the interactions between these subsystems increase, which in turn makes showcasing the system a challenge. A DSM allows the user to aesthetically scale up the subsystem's and its interactions in a format that is easier to comprehend.

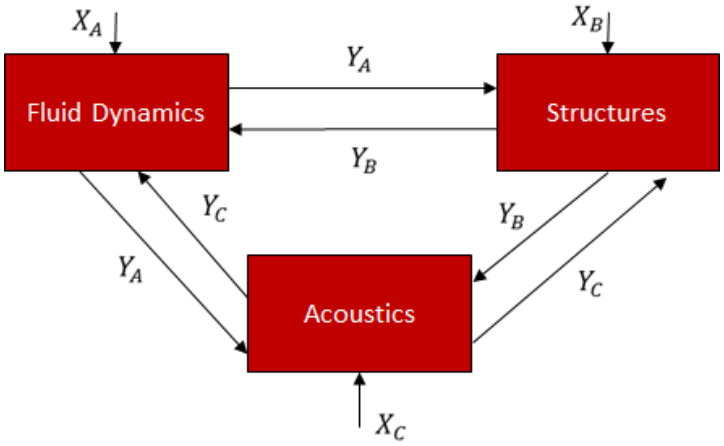

Figure 5. *Coupled System*

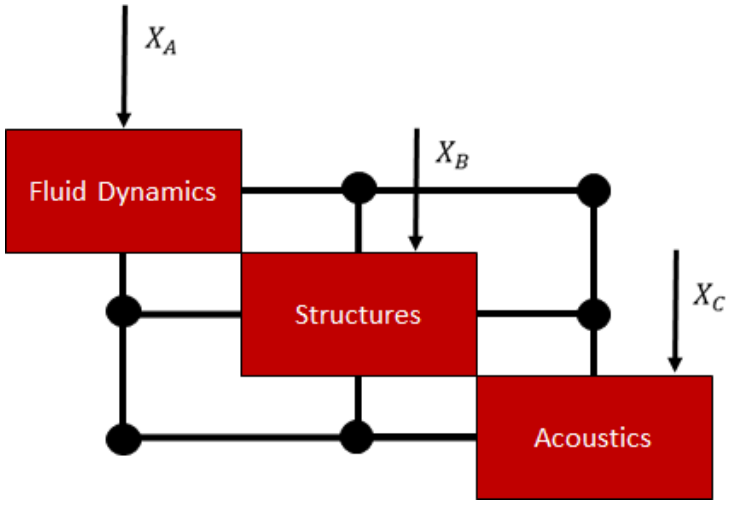

Figure 6. *Design Structure Matrix of Coupled System*

Global Sensitivity Equations

The Global Sensitivity Equation (GSE) is used to obtain the impact a design variable has on the system's response. This is done by obtaining the first order sensitivity of the systems behavioral response with respect to the systems design variables [16,51,52]. Once the sensitivity information is captured, a linear approximation to the behavioral response can be constructed,

which is later used in the optimization process for the design in MDO. A simplified 2 subsystem example is provided below in Figure 7.

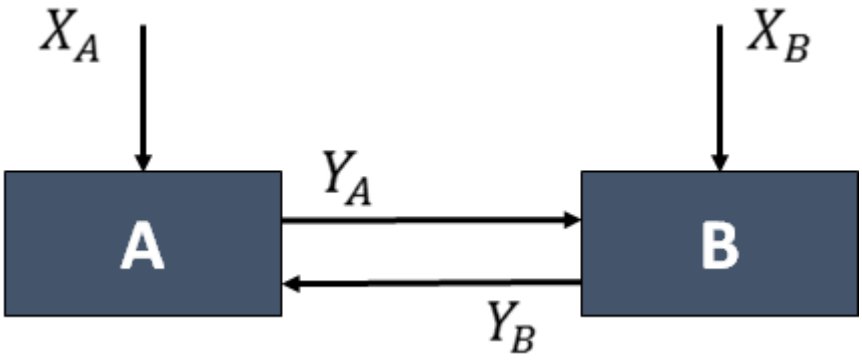

Figure 7. *Coupled Subsystem Example*

Here subsystem A and subsystem B are coupled together, whereXAand XB represent the design variables going into each respective subsystem andYAandYBrepresent the behavior variables of its respective subsystem. The behavior variables also act as inputs to the opposite subsystems, i.e.YAwill feed into subsystem B andYBwill feed into subsystem A. To find the total derivatives of the design variables a Taylor Series expansion is used shown by Eq. 1 and 2:

$$\frac{dYA}{dXA} = \frac{\partial YA}{\partial XA} + \frac{\partial YA}{\partial YB}\frac{dYB}{dXA} \tag{1}$$

$$\frac{dYB}{dXB} = \frac{\partial YB}{\partial XB} + \frac{\partial YB}{\partial YA}\frac{dYA}{dXB} \tag{2}$$

When the chain rule is applied the last total derivatives are found using Eqs. 3 and 4:

$$\frac{dYB}{dXA} = \frac{\partial YB}{\partial YA}\frac{dYA}{dXA} \tag{3}$$

$$\frac{dYA}{dXB} = \frac{\partial YA}{\partial YB}\frac{dYB}{dXB} \tag{4}$$

Once the equations are derived they can be represented in matrix form shown by Eq. 5 below:

$$\begin{bmatrix} 1 & \frac{-\partial Y_A}{\partial Y_B} \\ \frac{-\partial Y_B}{\partial Y_A} & 1 \end{bmatrix} \begin{bmatrix} \frac{dY_A}{dX_A} & \frac{dY_A}{dX_B} \\ \frac{dY_B}{dX_A} & \frac{dY_B}{dX_B} \end{bmatrix} = \begin{bmatrix} \frac{\partial Y_A}{\partial X_A} & 0 \\ 0 & \frac{\partial Y_B}{\partial X_B} \end{bmatrix} \tag{5}$$

The left hand side of the equations represents the sensitivity matrix, where the local behavior variables impact on a subsystem is captured. If a behavior variable changes in subsystem A its impact on subsystem B is captured with this matrix. The far right hand side matrix represents the sensitivity of the subsystem behavior variables with respect to the subsystems design variables i.e changes in design variables XA's impact on behavior variable YA. The total local derivatives are then solved for using matrix math to obtain the matrix shown in the center of the equation above. This matrix represents the total local sensitivity of a subsystem's behavior variables with respect to the design variables, including the coupling sensitivity captured in the left hand side matrix [51,52]. The local sensitivities within these matrices are typically found using a finite difference method.

The outputs found in the matrices can also vary highly by magnitude, as the units for most of the coupled systems won't match up. To get an accurate comparison of the strength these sensitivities have with respect to each other a normalization technique is used to normalize the left hand side matrix. Below is an Eq. 6 which represents the normalized coupling sensitivity equation of the 2 subsystem example shown above:

$$\frac{\partial YA'}{\partial YB} = \frac{dYA}{dYB}\frac{YB}{YA} \tag{6}$$

Once normalized, the inverse of the matrix can be multiplied with the right hand equation to calculate the total derivatives. To recover the true total derivative information the normalization process has to be reversed as shown below with Eq. 7.

$$\frac{dYA}{dXB} = \frac{dYA'}{dXB}\frac{YA}{XB} \tag{7}$$

Local Sensitivity Coupling Strength Analysis

Once the local sensitivity information is captured a comparison of coupling strengths can be made. This information can be important to determining strong and weak interactions within the localized design space. Once solved the GSE equations shown above provide the normalized sensitivity information. A method to analyze the sensitivity of these couplings is by measuring the normalized local sensitivity information and running a comparative study where a larger number represents a stronger coupling. By comparing the couplings the designer can get a general idea of the relative strength of each coupling within the local design space [17,51]. The designer can then select the couplings that are weak with little impact on the problem and consider elimination or suspension to save on computation time. This method is used later on to determine the coupling strengths that impacted T/O on the Ares 1.

Impact of Coupling Suspension on Objective Function

The previous section discussed finding the impact of local couplings and identify their strengths with respect to each other. Using the equations shown above a method can be derived to find the impact an elimination of a coupling has on the total value of a system in terms of the value function. To simplify the methodology the above GSE equation will be re-written in the following form:

$$[A]\left[\frac{dY}{dX}\right] = \left[\frac{\partial Y}{\partial X}\right] \tag{8}$$

Here the matrix [A] represents the sensitivities of the subsystem outputs with respect to the subsystem inputs, dY/dX represents the total derivative matrix, and the right hand side of the

equations represents the subsystem outputs with respect to the subsystem inputs. The partial derivatives of the total derivative matrix with respect to an element [A] can be found with Eq. 9 shown below.

$$[A]\frac{\partial}{\partial A_{ij}}\left[\frac{dY}{dX}\right] = -\left[\frac{\partial A}{\partial A_{ij}}\right]\left[\frac{dY}{dX}\right] \tag{9}$$

Here Aij represents the coupling that is being evaluated where A/Aij represents a unity matrix that is 0 everywhere except at the location of Aij where it is 1. Using Eq. 9 provides a good basis for comparison of a couplings strength against the total derivative, however to find the impact elimination has on the value function a quantifying measure is needed. Eq. 10 is presented below as a simplification of Eq. 9

$$\frac{\partial}{\partial A_{ij}}\left[\frac{dY}{dX}\right] \tag{10}$$

Eq. 10 represents the sensitivities of the total derivative with respect to each individual coupling Aij. Eq. 10 can then be further derived and represented by Eq. 11 shown below.

$$\frac{\partial}{\partial A_{ij}}\left[\frac{dY}{dX}\right] = \frac{\partial\left(\frac{dY_m}{dX_n}\right)}{\partial A_{ij}} \tag{11}$$

Here Ym represents the output from subsystem m, and Xn represents the design variable n. If a coupling is removed the change in Aij goes from unity to 0. This relationship yields the following relationship represents by Eq. 12 below.

$$\Delta\left(\frac{dY_m}{dX_n}\right) = \frac{\partial\left(\frac{dY_m}{dX_n}\right)}{\partial A_{ij}}\left(-A_{ij}\right) \tag{12}$$

Eq. 12 accounts for information changes in the linearization problem; to capture the relationship between the value function and total derivative the Eq. 13 is used.

$$\Delta\left(\frac{dF}{dX_n}\right)_{Y_m} = \Delta\left(\frac{dY_m}{dX_n}\right)\left(\frac{dF}{dY_m}\right) \tag{13}$$

Eq 13. finds the change in the value function with respect to design variable Xn when the coupling Aij is suspended or eliminated. If the change in Xn can be predicted than a prediction in the change of of the objective function in, the following cycle due to changes in the total derivative can be made when Aij is suspended with Eq. 14 below.

$$\Delta F_{X_n Y_m} = \Delta\left(\frac{dF}{dX_n}\right)_{Y_m} \Delta X_n \tag{14}$$

Eq. 14 gives the absolute change in the value function and will be used to determine the changes in the proposed value function in Chapter 6 of this research with respect to the coupling derivatives found in Chapter 5.

Thrust Oscillation

As mentioned in the intro Thrust Oscillation (T/O) will be discussed in great detail as this was the main contributing factor to the Ares 1 event and is the unanticipated behavior that the research focuses around [48]. T/O is a well-known phenomenon that occurs in SRM's and is caused by a combustion instability within the engine. The origins of the instabilities originate from fluid flow turbulence and acoustic energy that combine and cause a structural response of the rocket. If the energy states within are low the structure will respond by dampening out the increased energy and returning back to steady state. However in the case when these energy levels exceed the structure's ability to dampen, the structure responds with heavy vibrations and resonates

with the unsteady flow and acoustic energy. A simplified example of a spring mounted body is showcased in Figure 8 below to better understand the physics behind T/O.

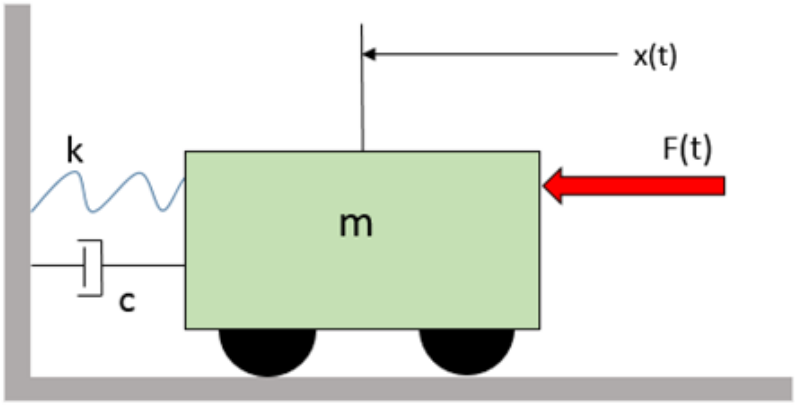

Figure 8. *Simple Spring-Mass System*

In the above example a forcing function represented byF(t)is placed onto a mass m which is held together by a springkand dampenerc. The forcing function acts as the energy that is provided into the system from the fluid flow turbulence and acoustic energy in the rocket example mentioned above. If the energy provided to the system from the forcing function is low the energy will be dampened out by the dampener, where the loads will cause minor deviation in the x direction, shown byx(t), and eventually return to a steady state. However if the energy provided exceeds the energy that the dampener can dampen, then the mass will have greater deviations in the x direction, where the loads can possibly cause structural harm to the mass. The worst case scenario will include so much excitation to the system that the dampener and spring break causing the mass to move into the wall or be flung in the opposite direction.

Much like the example mentioned above with the forcing function, the fluid flow turbulence and acoustic energy in a rocket combine to form an oscillatory pressure on the rocket structure known as pressure oscillation. Pressure oscillations within rocket engines are formed from 2 main phenomenon. The first being turbulent fluid flow that is typically caused by an

obstruction in the flow. The obstruction creates high and low pressure regions known as pressure vortices that oscillate back and forth in a phenomenon known as Vortex Shedding [32]. The frequency of the vortex shedding can cause structural instability if it were to coincide with the resonance frequency of the structure. Harmonic oscillations from the flow would then drive the structure to resonate, and in some cases cause vibrations that pose a threat to the structural stability of the object.

The second phenomenon that contributes to the creation of pressure oscillations within a SRM is the generation of acoustic waves and its relation to the acoustic-mode frequencies of the motor cavity. Acoustic waves are longitudinal waves that propagate throughout the engine in a compressive and decompressed state. The waves are released from the aft end of the motor chamber and propagate through. The propagation of the waves causes air particles to clash against the walls where the rate at which the waves collide with the walls can be recorded as a frequency. A simplified example would be the use of a wind instrument such as a saxophone. An initial flow of air propagates through the chamber of the instrument, colliding with a wall at a specific rate. The rate at which these particles collide produce acoustic waves that propagate throughout the instrument and produce musical notes. Geometry changes or changes to the speed of fluid flow to the instrument can be made to produce varying frequencies and sounds. Similarly any closed tubing geometry, such as a SRM can produce these acoustic waves. Three types of acoustic resonance can be produced by a tubed geometry, they are referred to as acoustic modes and are the longitudinal, Tangential and Radial modes. Figure 9 below showcases the varying modes, where the red showcases a positive pressure and the blue a negative pressure.

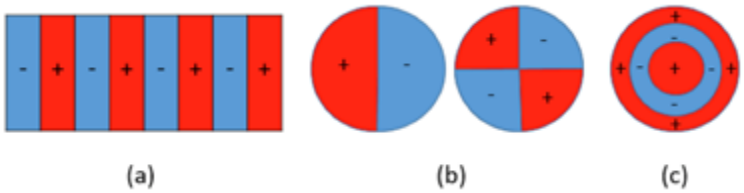

Figure 9. *(a) Longitudinal, (b) Tangential, and (c) Radial Modes*

Pressure Oscillations occur when the vortex-shedding frequencies caused by obstructions in the flow coincide with the acoustic modes of the engine chamber [23]. Once pressure oscillations within the chamber are generated the rockets structure will respond to these loads in various ways. Much like in the example above, pressure oscillations within an engine act as the forcing function did for the mass spring problem. In the case of a rocket engine the structure acts as the dampener; if the pressure oscillations are weak the engine will dampen out the loads and return to steady state. However, if these loads are strong the engine will respond with large vibrations that can propagate throughout the rocket. The response to the pressure oscillations within an engine chamber of a rocket is known as Thrust Oscillation.

T/O is a well known phenomenon that affects all rocket engines. Typically, these oscillations are dampened out by the rocket in various ways and cause no structural harm or major propagation issues. However, in the case of the Ares 1, it was noted that the pressure oscillation frequencies within the engine were close to the engine structures resonance frequency. Resonance is a phenomenon in which a vibrating system or external force like pressure oscillation drives another system to oscillate with large amplitudes [22]. The resonance frequency of an object is then the frequency at which these large amplitudes occur. It must be noted that the driving force doesn't have to be large to create a large amplitude oscillation from the system due to the storage of vibrational energy [22].

The frequency of the driving force doesn't need to have the exact frequency of a structure's resonance to have a similar impact. While the exact frequency causes the greatest oscillatory response from the system, the system can still respond with large oscillations due to transmissibility. Transmissibility is the capability of an external force to impact an oscillatory response of a system through the proximity to its resonance frequency [22]. Eq. 15 below describes this processes and showcases how even frequencies close to the resonance of a system can have a significant impact to the creation of a large amplitude response.

$$T = \frac{F_T}{F_O} = \frac{\sqrt{1 + \left(2\zeta \frac{\omega_i}{\omega_n}\right)^2}}{\sqrt{\left(1 - \left(\frac{\omega_i}{\omega_n}\right)^2\right)^2 + \left(2\zeta \frac{\omega_i}{\omega_n}\right)^2}} \quad (15)$$

Where Ft represents the force as a function of frequency, FO is the original force magnitude, is the damping coefficient, Wi is the vortex shedding frequency, and Wn are the acoustic modes.

As the frequency generated by an external force approaches the resonance frequency of the system its transmissibility goes to infinity, this is where the system will have the greatest oscillatory responses. In Figure 10 below transmissibility is plotted with the frequency ratio, where again it is shown that the external force does not need to be at the resonance frequency to have an impact on the system. It is then in the best interest of design engineers to avoid having the pressure oscillation frequencies within a rocket engine be close to its resonance frequency.

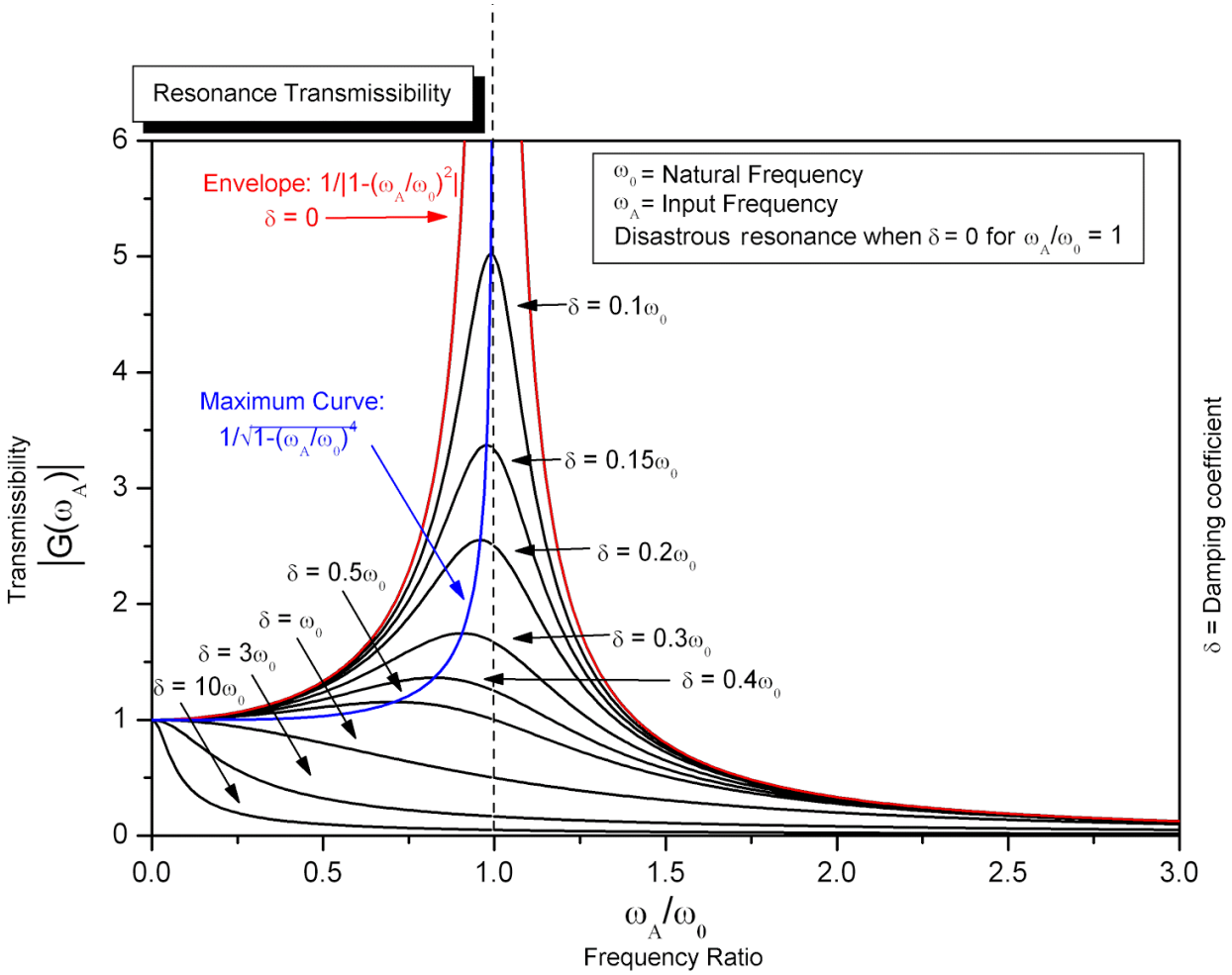

Figure 10. *Resonance Transmissibility provided by Katsuhiko Ogata (2005). System Dynamics (4th ed.). University of Minnesota. p. 617.*

In the case of Ares 1 the pressure oscillation frequencies within the engine chamber were close to the engine's resonance frequency causing a larger amplitude from T/O then expected. NASA formed a T/O mitigation team that concluded that the structures response was at first deemed insignificant to model but became the underlying factor in causing T/O. A means of capturing the significance of these couplings could have provided a means for the design engineers at NASA to capture this feedback and implement design changes before manufacturing of Ares 1. Chapter 4 covers a simplified means of modeling T/O and capturing subsystem feedbacks with the goal of capturing these unexpected behaviors during the design phase.

CHAPTER 4

MODELING THRUST OSCILLATION

Fluids Modeling

The modeling of the T/O event experienced by the Ares 1 is broken down into 3 subsystems: fluids, structures and acoustics. Each subsystem is modeled separately and the methodologies are covered in this chapter. To ensure accuracy an engine model from Zhang Q.'s "Theoretical Modeling and Numerical Study for Thrust-Oscillation Characteristics in Solid Rocket Motors" is used to compare numerical results [3]. In Figure 11 below the engine model with its dimensions in meters are shown. An inhibitor is added to determine impacts it has on creating vortex shedding in the engine.

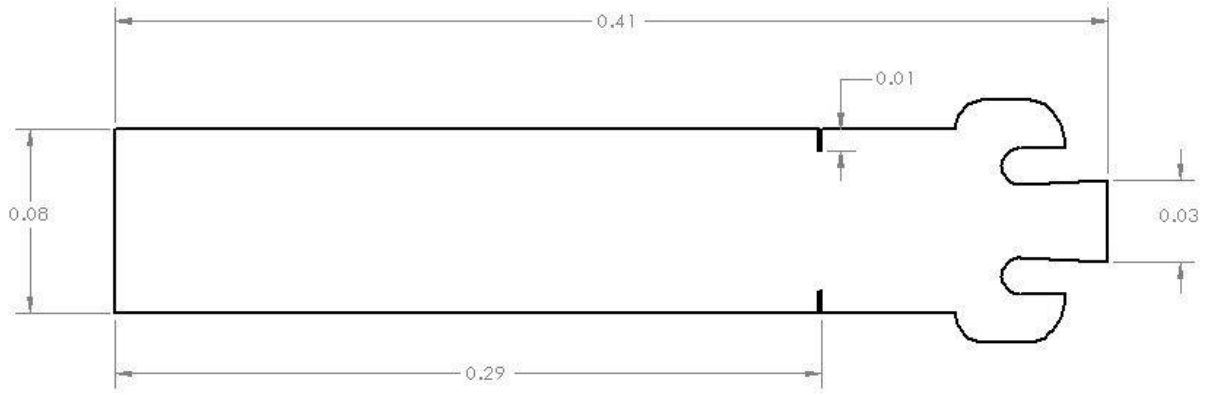

Figure 11. *Simplified Rocket Model with Dimensions in Meters*

Within the fluids subsystem a means to model the vortex shedding and turbulent flow within the engine chamber using a Computational Fluid Dynamics (CFD) method is presented. The goal of the fluids simulation is to solve for the vortex shedding frequency that is produced from a protrusion in the flow, in the model above this is the inhibitor. Star-CCM+ [24] is the CFD program being used to model the engine and capture the vortex shedding frequency. Within Star-CCM+ a static cold flow test is used to solve for the fluid physics. Static cold flow tests are typically done to verify the integrity of a propulsion system, and do not incorporate firing of the

engine [25,26]. This means that the combustion process is not accounted for during the Star-CCM+ simulation, which for the simplified model is a reasonable approximation.

To account for vortex-shedding within the simulation an implicit unsteady time model is used. Vortex Shedding is a time dependent process where turbulent flow around the engine changes drastically with time. Using the implicit time model vortex shedding can be modeled around the inhibitor and a frequency, which is also a time dependent variable, can be captured. The time step that is determined needs to be at most half to the expected frequency of the vortex shedding produced. To approximate the vortex shedding frequency Strouhal's number which is presented in Eq. 16 is used. Strouhal's number captures the frequency of vortex-shedding f based off of the fluid's velocity U, and obstacle length L[29].

$$St = \frac{fL}{U} \tag{16}$$

By using Eq. 16 a period approximation of 1 millisecond is not expected from the vortex-shedding frequency, yet a more conservative time of .1 millisecond is chosen in case the approximation has a large deviation of error. Once time within the simulation is set, Star-CCM+ requires a flow regime to be selected, which for the case of T/O the turbulent flow viscous regime accounts for the expected physics within the engine. Within the engine chamber the turbulent flow that is important to capture is at and behind the inhibitor. In an attempt to save on computational time Star-CCM+ has a modeling technique called detached eddy modeling [24]. Eddy in fluid dynamics is the swirling of fluid that is created when fluid flows past an obstacle [27,28]. Vortex-shedding itself is a type of eddy flow. Using a detached eddy model the target of interest, which is at and near the inhibitor can be modeled using large eddy simulations gathering a more accurate result. The flow near the beginning of the rocket engine can then be modeled using Reynolds-Averaged Numerical Solution (RANS) which is used for ideal flow. By splitting the flow up into

2 regions, before and after the inhibitor, and changing the modeling techniques between each region the model can ensure accuracy when capturing the vortex shedding frequency while also saving computational time during ideal flow regions [24]. Figure 12 showcases the varying pressure regions within the simplified rocket model. A darker shade of blue represents low regions of pressure, while higher shades of red represent high pressure regions. Vortex shedding can be seen coming off the inhibitor walls.

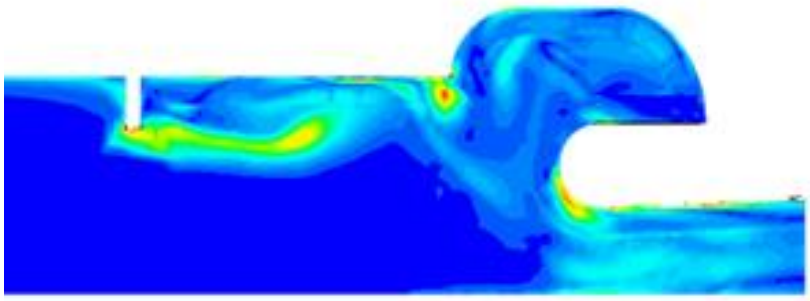

Figure 12. *Star-CCM+ Pressure Regions of Simplified Rocket*

The analytical process is then started by first using a coarse mesh of the engine model and implementing a longitudinal force monitor on the inhibitor. The force monitor is used to capture the vortex-shedding frequency caused by the shedding of vortices around the inhibitor, which in turn changes the pressure field in the region and applies an oscillatory force onto the inhibitor. This oscillatory force has the same frequency as the shedding of vortices behind the inhibitor which coincides with the vortex shedding frequency. Figure 13 below shows the force monitor loads that the inhibitor underwent in the CFD simulation. Once a solution is found the vortex-shedding frequency is obtained from the oscillatory load and the simulation is then reran with a finer mesh.

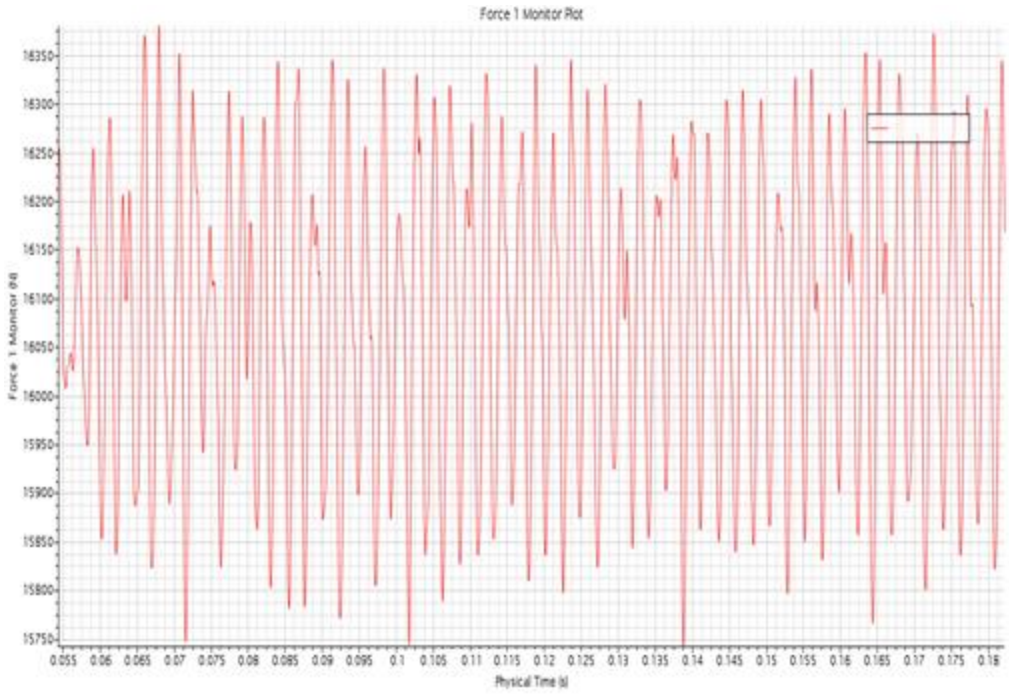

Figure 13. *Star-CCM+ Force Monitor Loads in Newton's*

The vortex-shedding frequency solution captured by Star-CCM+ is shown in Figure 14 where X in the legend represents the natural frequency and Y the amplitude.

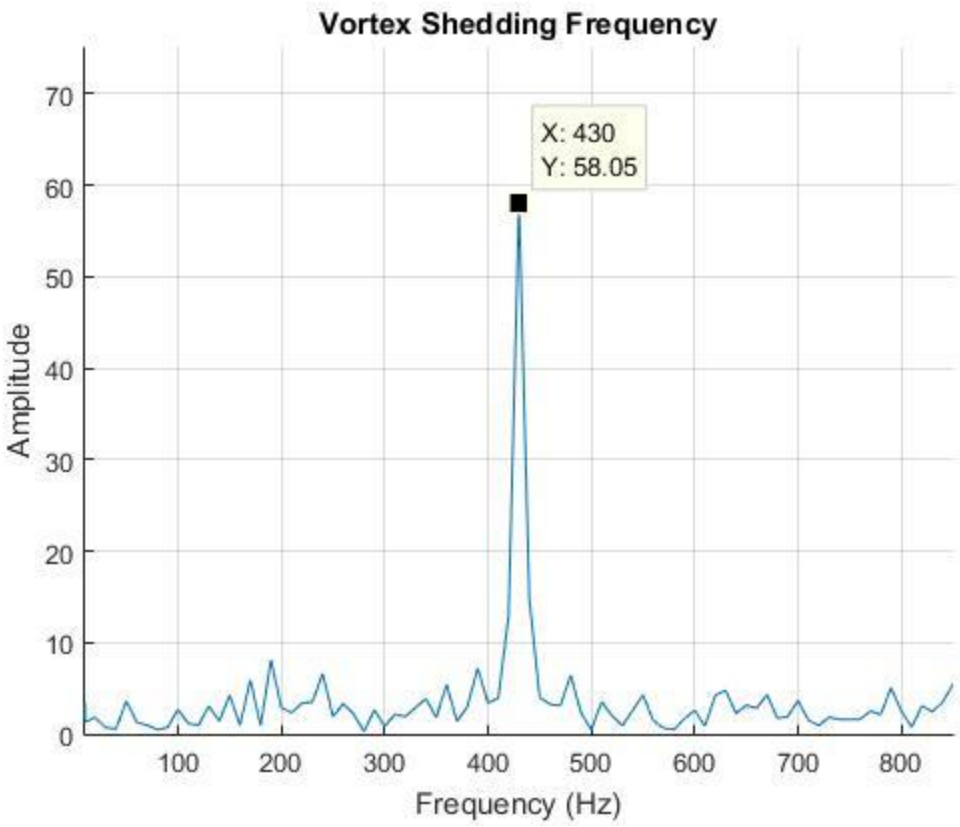

Figure 14. *Vortex Shedding Frequency Produced by Inhibitor*

The loads applied to the walls by pressure oscillation are also captured using the force monitor, where the longitudinal force is placed on key nodes in the structures simulation. Using this method and the input variables given by Zhang Q. it was determined that the simulation for capturing vortex shedding frequencies had a high level of accuracy and can be scaled up to the Ares model.

Acoustics Modeling

Modeling of the acoustic subsystem is done numerically with the aim of determining the acoustic mode frequencies of the SRM. The analysis is done with the assumption that the cavity of the engine is treated as an acoustically closed system despite the exit area coming into contact with the external environment [18]. The assumption needs to be made for a theoretical method to be used, which also provides an added benefit of saving computational time during system

convergence. As mentioned before in the previous chapter there are 3 main acoustic modes of an acoustically closed engine, the longitudinal, tangential and radial modes shown in Figure 9. All three acoustic modes may contribute to acoustic instabilities within engines, but it is noted that tangential and radial modes show higher instabilities at higher frequencies [19]. The Ares 1 was shown to have had very low acoustic and resonance frequencies associated with the rocket motor [46,47]. To simplify the problem the radial and tangential acoustic modes will be neglected in the model as they are more associated with higher frequencies, which did not show any contribution to T/O in the Ares 1. The model used by Zhang Q. will still be used as the longitudinal mode frequencies were a primary data point captured in their testing.

To find the acoustic resonance of the modeled engine the concept of standing waves will be briefly discussed. A standing wave is the vibrational state of a stable system where the wave is clamped between two fixed ends called nodes [21]. The standing wave modes arise from a combination of reflection and constructive interference. Reflection occurs when a wave hits a boundary and then changes phase, this phase change then causes constructive interference amplifying the peaks and troughs of the wave [21].

The wavelength associated with the standing wave describes the mode number. A half wavelength is associated with mode 1, and each subsequent mode has a increase in ½ wavelength i.e mode 2 will have a wavelength of 1. This is shown in Figure 15 below which is taken from the acoustic data of the simplified model.

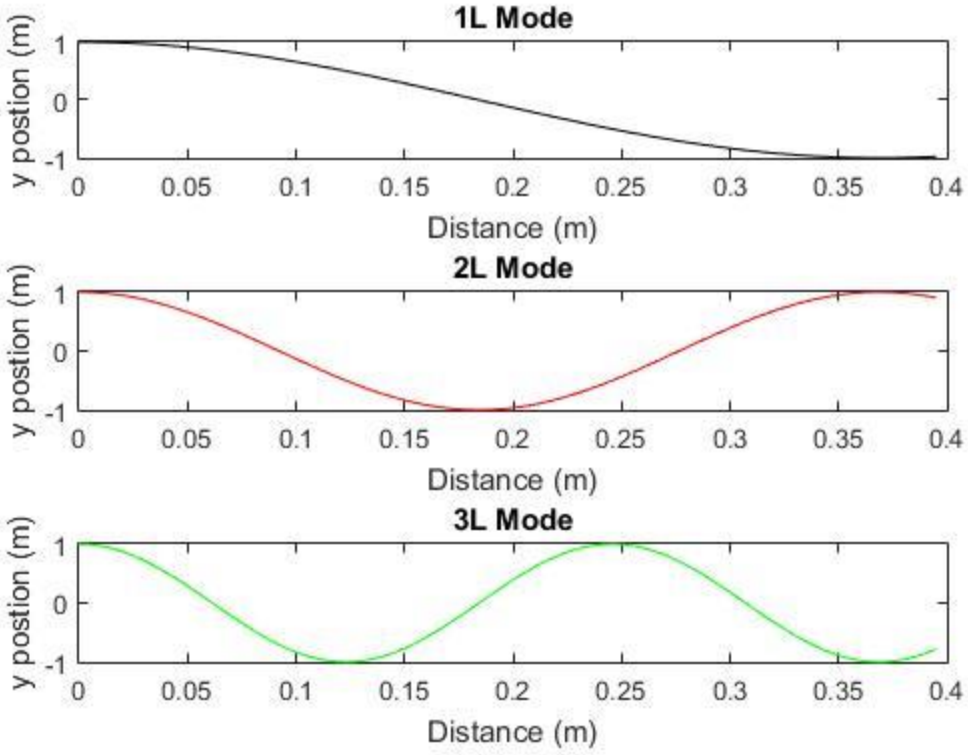

Figure 15. *Acoustic Wavelengths of the Simplified Model*

The resonance of a system is heavily depended on the first mode, also known as the fundamental tone with each subsequent mode having a smaller amplitude and impact on resonance [21]. In most cases the first 3 acoustic modes are adequate in capturing the resonance and response of a closed acoustic system. Therefore calculating the frequency of the first 3 acoustic modes within the engine model is crucial to determine resonance. In the case of rocket engines, Eq. 17 below shows good experimental and theoretical agreement in solving for the natural frequencies of an acoustically closed system [20].

$$f_{lmn} = \frac{c}{2\pi}\sqrt{\frac{k^2\pi^2}{L_c^2}} \tag{17}$$

In Eq. 17 c is defined as the speed of sound, LC is the length of engine chamber, and k is the longitudinal acoustic modes. Speed of sound is heavily dictated by the temperature of the surrounding gas and is described by Eq. 18 below.

$$c = \sqrt{\gamma RT} \tag{18}$$

Here in Eq. 18 is defined as gamma, which represents the ratio of specific heats, R represents the gas constant, and T represents the temperature of the gas.

Higher temperatures and density play a major role in determining the speed of sound in a specific medium [22]. In the case of Zhang's model a temperature of 20 degrees Celsius and gas constant of 1.4 is used to give a speed of sound of 343 m/s. With all variables accounted for, Table 1 showcases the natural frequencies of the simplified model:

Table 1. *Acoustic Mode Frequencies for SRM chamber*

Acoustic Modes	Experimental Data	Zhang's Model	% Error
1L	425.262 Hz	410 Hz	3.72
2L	850.523 Hz	875 Hz	-2.80
3L	1275.78 Hz	1280	-0.33

Compared with the analysis done by Zhang the simplified numerical model had close frequencies with errors of at most 3.72%. Going forward this acoustic method will be used for the Ares 1 model for its ease of convergence and high accuracy. Temperature changes will be accounted for in the Ares 1 model to ensure good experimental and theoretical correlation.

Structures Modeling

When the acoustic mode frequencies are captured and compared with the vortex shedding frequencies, pressure oscillations can then be generated and placed onto the interior walls of the engine. The pressure oscillations are simulated in ANSYS workbench [31] as a sinusoidal forcing function. To simulate the acoustic impact on the engine a Harmonics Response Analysis (HRA) is

used to capture the effects of resonance. HRA is an analysis technique that is used to determine the steady-state response of a structure to loads that vary sinusoidally with time. This analysis tests to determine the deflections the structure would undergo and enables a designer to determine if the system can overcome the forced cyclical loads [22]. To simulate the loading conditions that are placed on the engine structure the forcing monitor used in Star-CCM+ and the range of frequencies found from vortex shedding and the acoustic modes are used. Figure 16 shows the loads being applied to the inhibitor in ANSYS as a sinusoidal function taken from the Star-CCM+ simulation. The loading conditions of the model also consist of 2 displacements bounds at the far left end of the simplified engine. These resemble the connection points of the engine to the remainder of the rocket.

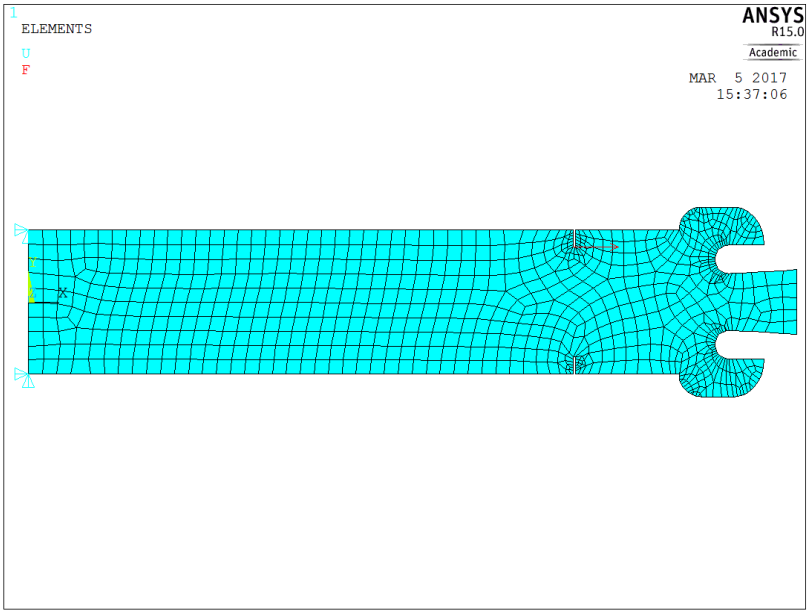

Figure 16. *ANSYS Simplified Model*

Taking these base loads then applying the basic harmonics excitation, shown below in Eq. 19, can capture the pressure oscillation loads on the engine [22].

$$f(t) = F_o \sin(wt) \tag{19}$$

In Eq. 19 FO represents the magnitude of the force, w represents the driving frequency and t represents time.

The amplitude is found from the forcing monitor placed on the inhibitor during the CFD process and is the maximum load experienced by the inhibitor, the loads are also shown in Figure 13. Within the ANSYS software package 3 types of solution methods are offered. The full, reduced and mode superposition methods. All three solutions use the sinusoidally driven harmonic oscillator equation, described below in Eq. 20 and Eq. 21 [22]:

$$\ddot{x}(t) + w_n^2 x(t) = f_0 \cos(wt) \tag{20}$$

$$f_0 = \frac{F_o}{m} \tag{21}$$

In Eq. 20 x represents the displacement, Wn represents the natural frequency, and t the time. Eq. 21 represents the magnitude of the force FO over the oscillatory mass m, which for the simplified engine is the mass of the engine.

The full method uses the full matrices to calculate the harmonic response, and is the analysis method used for the simplified engine. The matrices that are used within the ANSYS package use the beam matrix method and is created through the meshing criterion set by the user [31]. Once the meshing is completed and the loads applied the analysis can be ran and engine deflections captured. Figure 17 below showcases the inhibitor deflections after the simulation was ran.

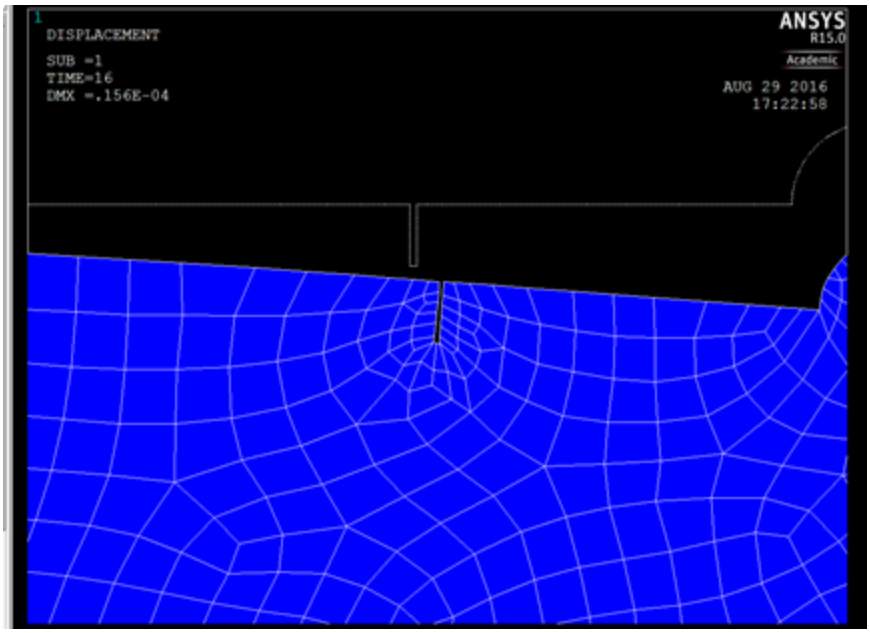

Figure 17. *ANSYS Simplified Model Showcasing Deflections of Inhibitor*

The deflection measured is the maximum deflection in meters as a subset of 16 time steps. Its represented in Figure 17 as DMX and represents .156e-4 meters of deflection. This small deflection is consistent with the size of the engine shown in Figure 11. The motor itself propagates back and forth throughout the 16 time steps with the material properties of Aluminum chosen for this simulation. Typically in solid rocket motors an alloy of Titanium and Aluminum is used [33,38].

Deflection of the inhibitor is a key point of interest as any length change will alter the vortex-shedding frequency produced by the inhibitor. An increase an inhibitor length will cause the vortex shedding frequency to logarithmically decrease, while a shortening of the inhibitor length will cause the vortex shedding in the engine to logarithmically increase [34]. This small interaction is key to determining the T/O event in the Ares 1 as the deflection in the engine chamber and inhibitor was deemed small and inconsequential to system success. To capture the impact a deflection in inhibitor length has on the creation of thrust oscillation the nodal displacements are captured and used to simulate changes in vortex shedding frequencies in Star-CCM+. This is done

by importing the deflected ANSYS model back into Star-CCM+ where the CFD simulation is ran and new vortex shedding frequencies are gathered. The frequency range is then compared with the acoustic modes and the new model, with a deflected inhibitor, is placed back into ANSYS. New loading conditions are placed back onto the structure and a HRA is ran again to determine the new deflections of the engine. This is done until convergence is met and the frequency of vortex shedding change is miniscule.

Lower Fidelity Model

It was noticed during system convergence that the Star-CCM+ simulations would require 2-3 days of computational time to complete an iteration, which was heavily taxing. In an attempt to minimize computational time and still gather meaningful results a lower fidelity meta-model that used initialization conditions from Star-CCM+ was produced. The lower fidelity meta-model uses a numerical method to solve for the pressure oscillation forcing functions on the engine walls and calculates the vortex shedding frequency produced by the inhibitor. The main focus is to evaluate the change in deflection of the inhibitor and evaluate its impact on the frequency of vortex shedding. Below is the methodology for the lower fidelity meta-model and is designed around D.R Mason's numerical method for solving pressure oscillations and structural vibrations in space shuttle Reusable Solid Rocket Motors (RSRM) [30].

D.R. Mason's methodology has a similar approach to determine the loads placed on the structure as discussed in the structures and fluids section of this chapter. With the use of a dynamic pressure excitation throughout the engine at every ith location the forcing function can be determined with Eq. 22:

$$P_i(t) = \sum_j p_{ij} \sin(2\pi f_{ij} t) \tag{22}$$

Here the initial pressure pij is on a grid of i by j where fij represents the vortex shedding frequency and t the time. To determine the frequency of vortex-shedding, Strouhal's number is used based on the inhibitor length and fluid flow velocity of the engine. To simulate the randomness of pressure and oscillatory loads captured by Star-CCM+ on the inhibitor a random number generator is used to determine the random magnitude of loads. This process is shown in Eq. 23 below, where P high and P low are the high and low pressure loads captured by Star-CCM+ and rand represents a random real number between 0 and 1. The randomization of the magnitude of pressures attempts to capture the randomness of turbulent flow within the engine.

$$P_i(t) = \sum_j P_{ij} \sin\left(2\pi f_{ij} t\right) + rand([0:1]) * (P_{high} - P_{low}) \tag{23}$$

Eq. 24 below describes the natural frequency fij and is taken from Strouhal's Equation described in Eq. 16.

$$f_{ij} = \frac{S_{ij} U_i}{L_i} \tag{24}$$

With the equations in place the meta-model had to be tested with Star-CCM+ to ensure accuracy. Figure 18 below showcases the loads captured the numerical meta-model which can be compared with the loads captured in Star-CCM+ in Figure 13.

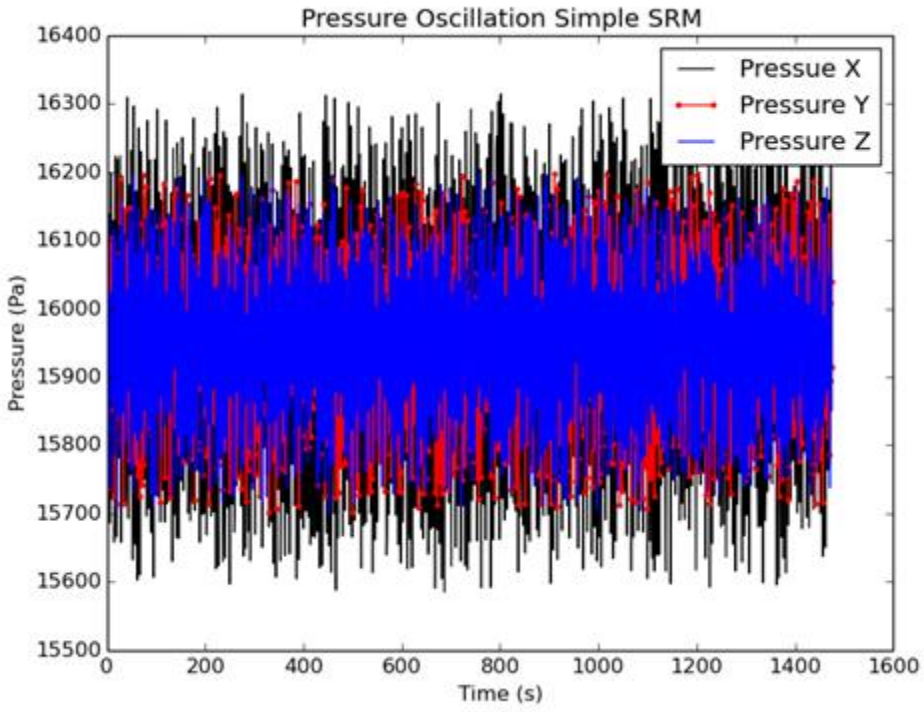

Figure 18. *Lower Fidelity Pressure Loads*

The pressure oscillation loads captured by the meta-model had a maximum deviation error of 3.8% from the loads captured by the Star-CCM+ simulation. This accuracy was within tolerance and to save on computational time will be used as a means to capture the pressure oscillation loads within the simplified engine and the Ares 1 model. A system architect for the meta-model process is showcased in Figure 19 below:

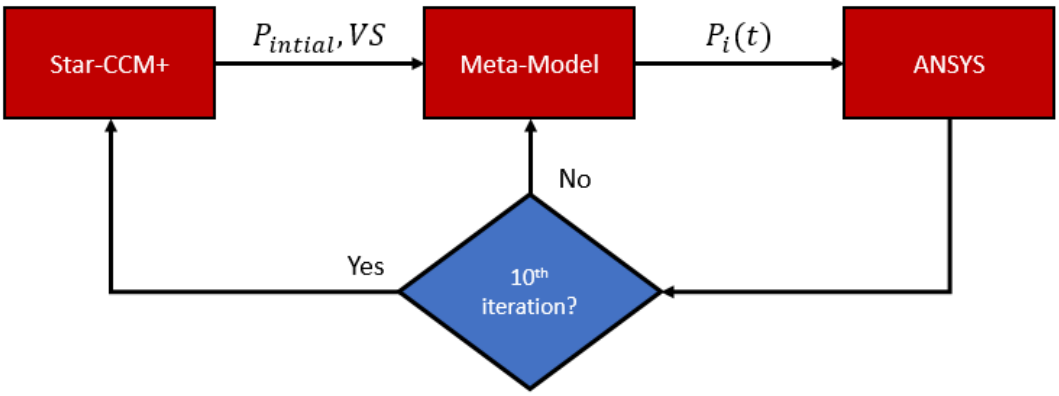

Figure 19. *System Architect with Meta-Model*

Star-CCM+ is used to initialize the model which sends the initialized pressure conditions and oscillatory flow information to the meta-model. This information is then passed on to ANSYS, where deflections are measured and then returned to the meta-model. The meta-model then captures the new pressure oscillation loads based on changes in inhibitor length and returns that information to ANSYS. Every 10th iteration the deflected model is sent back to Star-CCM+ to capture a higher fidelity reading of the fluid flow, which is then passed along to the meta-model and the process mentioned above repeats.

Once the pressure oscillations are captured a forcing function is defined and placed into ANSYS. It is noted that the pressure oscillation magnitude alone does not sufficiently capture the loads undergone by the structure. According to Dr. Blomshield, thrust oscillations within engines are almost always more severe than pressure oscillations [35,48]. Two equations were proposed by Blomshield to accurately capture the magnitude of the pressure oscillations on a solid rocket motor. The first described in Eq. 25 describes a lower fidelity calculation that gives a good approximation to the upper limits of thrust oscillation.

$$\Delta F = 2A_C \Delta P \tag{25}$$

Where F is thrust oscillations, Ac is the cross-sectional area of the engine chamber and P is the pressure oscillations in the chamber. The second equation proposed by Blomsheild is described by Eq. 26 below and gives a higher fidelity calculation to the pressure oscillation within an engine.

$$\Delta F = [F + P_A A_E - (\bar{P}_N + \bar{P}_H)A_C]\frac{\Delta P}{\bar{P}_N} \tag{26}$$

Where F is thrust oscillations Ac is the cross-sectional area of the engine chamber, P is the pressure oscillations in the chamber, F is mean thrust of engine, Ae is the exit area the engine nozzle, PA is the ambient pressure, PN is the nozzle end pressure, and PH is the head end pressure.

With the loads captured and the system architecture in place, the Global Sensitivity Equations can then be solved and evaluated to determine the local coupling strengths. The aim is to determine if the structures feedback from the models had a significant influence on the fluids subsystem which aided in the creation of thrust oscillation in the Ares 1.

CHAPTER 5

LOCAL SENSITIVITY ANALYSIS

Capturing the Global Sensitivity Equations

The proposed methodology to capture the Global Sensitivity Equations has been discussed in the background section of this research but will be reiterated here using the simplified rocket model as a guide. Once the local sensitivity matrix of the simplified model is found, the proposed modeling techniques showcased in Chapter 3 and the GSE methodology covered in Chapter 2 will be used for the Ares 1 model. A breakdown of varying design variables and finite difference lengths with be made on the Ares 1 model to capture the system's response. The initial step to finding the global sensitivity equations is to capture the design and behavior variables of the system. A system DSM of the simplified model is presented below in Figure 20 showcasing the key subsystems with their respective design and behavior variables.

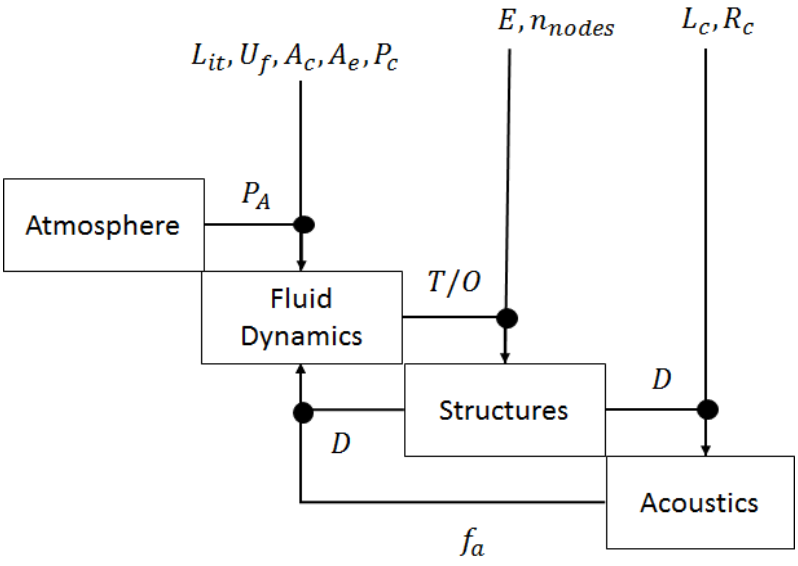

Figure 20. *DSM of the Simplified Rocket Model*

In Figure 20 the model is broken up into the 3 respective subsystems discussed previously, with the inclusion of Atmosphere which contributes the constant variable of ambient pressure to

the Fluid Dynamics subsystem. Table 2 goes over the design and behavior variables with their respective representations shown in Figure 20.

Table 2. *Design and Behavior Variables of the Simplified Rocket DSM*

Design Variables		Behavior Variables	
L_{it}	Length of Inhibitor	T/O	Thrust Oscillation Forcing Function
U_f	Velocity of Flow	D_X	Displacement in X
A_C	Area of Chamber	D_Y	Displacement in Y
A_e	Area at Exit	A_1	First Acoustic Mode
P_C	Pressure of Chamber	A_2	Second Acoustic Mode
E	Modulus of Elasticity	A_3	Third Acoustic Mode
n_{nodes}	Number of Nodes (taken from ANSYS)	f_{vs}	Vortex Shedding Frequency
L_C	Length of Chamber		

With the system architecture defined, a convergence test is conducted to ensure the physics is properly captured. If the convergence test failed the GSE's captured would be oscillatory in nature, not converge, and capture invalid results. The key points of interest that were evaluated are the changes in length of the inhibitor and the vortex shedding frequency as a function of time. Table 3 below covers the convergence test and showcases the number of iterations it took to reach convergence.

Table 3. *Convergence Test of the Simplified Rocket Model*

Time	**Iteration**	**Vortex Shedding**	**Inhibitor Length**
0-2 sec.	1	430 Hertz	.01 Meters
2-4 sec.	2	466.67 Hertz	.00899 Meters
4-6 sec.	3	381.82 Hertz	.01099 Meters
6-8 sec.	4	381.818 Hertz	.011 Meters
8-10 sec.	5	381.819 Hertz	.0109 Meters

Within 3 interactions the physics of the system showcased convergence with minor deviations in the 4th and 5th iteration. The vortex shedding frequency is once again measured in hertz and the inhibitor length in meters. It is interesting to note that even with such minor changes in inhibitor length large deviations in vortex shedding frequencies were captured. This is consistent with prior research showcasing large deviations at smaller inhibitor lengths [34,37].

Once the system is converged a finite difference method is used to propagate the design variables to evaluate the sensitivity matrix. The finite difference method is a numerical method that is used to approximate differential equations [36]. The approximation for the first derivative of a function "f" can be founds using Eq. 27 below.

$$f'(x) \approx \frac{f(x+h) - f(x)}{h} \tag{27}$$

Where h represents the discretization size of function f(x). A discretion size of 5% for each function was used, i.e. if the function for vortex shedding has f(x)=430 hzthen the discretization size chosen was 21.5. This was done for each function and used to calculate the local sensitivity matrix, also known as the A matrices. The A matrix is shown below in Eq. 28 and its correspondent matrix is shown in more depth in Eq. 5.

$$[A]\left[\frac{dY}{dX}\right] = \left[\frac{\partial Y}{\partial X}\right] \tag{28}$$

Within the first analysis of the simplified model the vortex shedding frequency was captured and passed on to the structures subsystems. The frequency would then be used within the structures calculation to evaluate pressure oscillations on the inhibitor walls. This was later changed for the Ares 1 Model as a more accurate prediction of T/O was found using Blomsheild's

equations [35]. The analysis was ran and the local sensitivity matrix A was found and is shown in Table 4 below.

Table 4. *A Matrix of Simplified Rocket Showcasing Local Sensitivities*

	f_{vs}	D_X	D_Y	A_1	A_2	A_3
f_{vs}	1	-0.0005	-0.0015	0	0	0
D_X	0.0993	1	0	0	0	0
D_Y	0.14369	0	1	0	0	0
A_1	0	-1.15E-5	0	1	0	0
A_2	0	-1.85E-5	0	0	1	0
A_3	0	-1.29e-5	0	0	0	1

Strong Coupling
Moderate
Weak Coupling

Table 3 is a breakdown of the impacts one behavior has on another when behavior variable. Columns represent the behavior variables that are being impacted on by the inputs of the rows. For instance the column fvs is the vortex shedding frequency and is impacted strongly by Dx and Dy which represent the displacement of inhibitor nodes in the X and Y direction. The values have been normalized to give a qualitative comparison of each behavior variables impact on anther. It is noticed that the feedback from the structures subsystem back onto the fluids has a moderate coupling in the simplified model. This moderate coupling represents the impact a change in vortex shedding frequency has on the displacement of the rocket i.e. the pressure oscillations produced in the engine have a moderate impact on structural displacement. This coupling while not significant would still carry some weight to a designer and cause a more in depth analysis of the structures feedback to system performance. It is also noted that small changes of displacement in the X direction also have an impact on the acoustic modes produced, but these are insignificant to the local acoustic subsystem.

Once the A matrix is found the total derivative matrix can be solved by taking the inverse of the A matrix and multiplying it with the local derivative matrix shown in Eq. 28. The total

derivative matrix shows the total impact a design variable has on a behavior variable, where all local changes are captured with the Taylor series expansion mentioned in the GSE background section of this research. Table 5 showcases the total derivative matrix and is a qualitative measure of the impact each design variable has on the local subsystem.

Table 5. *Total Derivative Matrix of Simplified Rocket*

	L_{it}	U_f	E	L_c
f_{vs}	-1.5E9	400.11	0	0
D_X	2.8	-7.37E-7	0	0
D_Y	20.178	-5.29E-6	0	0
A_1	0	-5.2E-4	0	-1.08E6
A_2	0	-1.6E-4	0	-4.2E6
A_3	0	-1.6E-3	0	-8.5E6

The design variable with the greatest impact on a subsystem is the length of the inhibitors contribution to the creation of vortex shedding in the fluids subsystem. The second biggest impact is the length of the rocket chambers contribution to the acoustic modes. It is noted that the modulus of elasticity had a very weak contribution to the systems behavior variables. The results are consistent with Zhang's model and were expected as the length of the inhibitor and chamber length have large contributions to subsystem outputs [3]. The local sensitivity analysis shows a moderate feedback from structures and lays out the importance of capturing these interactions. The methodology covered is now used for the Ares 1 rocket where a higher fidelity method was implemented and more design variables captured in the total derivative matrix. A comparative analysis of the impact the finite difference discretization size has on the sensitivity and total matrix values was also evaluated. All variables are normalized to protect ITAR data.

Local Coupling Analysis of the Ares 1

Before performing the Local Coupling Analysis two major changes to the evaluation of the Ares 1 model were made. The first major change was to use the T/O equations presented by Blomsheild to capture a higher fidelity reading of T/O's impact on local subsystems [35]. The changes incorporate engine geometry design variables that weren't captured before with the simplified rocket model. The second major change was taking out the Vortex Shedding frequency behavior variable as this just feeds into the pressure oscillation behavior variable which is then the cause of T/O. With the changes made the analysis was run for the Ares 1 model and used the same methodologies as discussed above with the simplified rocket model. The first analysis ran with the Ares 1 model used a discretization size of 5%. A specific length for the inhibitor was chosen that correlated to a vortex shedding frequency that was equal to the resonance frequency of the first acoustic mode. This was done to capture the greatest impact T/O can have on the local subsystem's and spot key design and behavior variables that contributed to the T/O event on the Ares 1. The A matrix for the first analysis of the Ares 1 model is shown below in Table 6.

Table 6. *A Matrix of Ares 1 Showcasing Local Sensitivity*

	T/O	D_X	D_Y	A_1	A_2	A_3
T/O	1	16.4211	-342.22	-334.2	-15.97	-10.05
D_X	84.9281	1	0	0	0	0
D_Y	458.331	0	1	0	0	0
A_1	0	-.4627	0	1	0	0
A_2	0	-.4627	0	0	1	0
A_3	0	-.4627	0	0	0	1

Strong Coupling
Moderate
Weak Coupling

The first major change noticed from the simplified model is the inclusion of the 3 acoustics modes impact on T/O. The inclusion of changes in geometry showcase how acoustics has a greater impact than previously captured on the simplified model. As the frequency of vortex shedding was

brought closer to the resonance frequency within the Ares 1 model the impact the length of inhibitor had on T/O had significantly increased. This is showcased in the first row where a normalized value of -342.22 for Dy shows a large coupling impact on T/O. This is consistent with prior research and reaffirms the value of doing a local couplings analysis to capture subsystem feedbacks. Another analysis will be made where the starting inhibitor height is further from resonance to detect if any major impacts to T/O occur. The total derivative information was then solved for and is presented in Table 7 below.

Table 7. *Total Derivative Matrix of Ares 1 Engine*

	L_I	U_f	P_C	A_C	A_E	E	L_C
T/O	-3.31E17	1.82E13	216.15	8.02E13	-2.0962E14	6.5E-17	1.4E6
D_X	4.67E7	-2.568E3	3.05E-8	-1.13E4	-2.96E4	0	-2.1E-4
D_Y	1.22E9	-6.719E4	-7.9E-7	-2.96E5	7.751E5	0	-.0055
A_1	2.07E9	-1.1371E5	-1.35E-6	-5.02E5	1.31E6	0	4.224
A_2	4.144E9	-2.274E5	-2.7E-6	-1.0E6	2.62E6	0	-16.87
A_3	6.2159E9	-3.41E5	-4.05E-6	-1.5E6	3.93E6	0	-37.96

With the capturing of geometrical changes in the Ares 1 model the acoustic behavior variables show greater impact from variables that had little or no impact before. For instance the length of the inhibitor impacts the magnitude of T/O, which eventually impacts the displacement in the X direction causing changes to the acoustic modes. It is interesting to note how slight changes in engine design can severely impact the magnitude of T/O. For instance the length of the inhibitor has had the greatest impact, but slight changes in velocity, Area of chamber and Area at exit are also major contributors to T/O within the rocket engine. The design variable that had the least impact on any behavior variable was the modulus of elasticity.

The next analysis that is proposed is a change in the finite difference method discretization size. The first analysis was done at 5% of the functions starting value, i.e. if the inhibitor has a

length of 100 meters the discretization size would be 5. The analysis proposed is done at a discretization size of 10 % and the A matrix for this analysis is shown in Table 8 below.

Table 8. *A Matrix of Ares 1 with a 10% Discretization Size*

	T/O	D_X	D_Y	A_1	A_2	A_3
T/O	1	8.4741	174.696	-371.5	-28.41	-18.86
D_X	87.4259	1	0	0	0	0
D_Y	517.044	0	1	0	0	0
A_1	0	-.2428	0	1	0	0
A_2	0	-.2428	0	0	1	0
A_3	0	-.2428	0	0	0	1

Strong Coupling
Moderate
Weak Coupling

Notable changes noticed with an increase in discretization size are the magnitude changes of displacement in the X and Y in the first row. This represents the displacements impact onto T/O and shows a magnitude decrease of roughly a half. This is consistent with prior research showcasing how volatile small changes in inhibitor length can have on the creation and magnitude of T/O [34]. These drastic changes represent the nonlinearity of the displacement functions captured. Magnitudes of the other derivatives stayed relatively consistent with the change in discretization size.

Table 9 below showcases the total derivative matrix of the analysis with a 10% discretization size.

Table 9. *Total Derivative Matrix of Ares 1 with a 10% Discretization Size*

	L_I	U_f	P_C	A_C	A_E	E	L_C
T/O	-5.35E17	1.55E13	363.19	1.41E14	-3.75E14	6.6E-17	4.01E6
D_X	7.8E7	-2.267E3	-5.29E-8	-2.05E4	5.4668E4	0	-5.86E-4
D_Y	2.23E9	-6.5E4	-1.51E-6	-5.88E5	1.56E6	0	-.0168
A_1	1.81E9	-5.258E4	-1.22E-6	-4.76E5	1.26E6	0	-4.03
A_2	3.62E9	-1.051E5	-2.45E-6	-9.52E5	2.53E6	0	-16.12
A_3	5.43E9	-1.577E5	-3.684E-6	-1.42E6	3.8E6	0	-36.25

The total derivative matrix captured above in Table 8 shows small deviations in magnitude from the derivatives captured in Table 7. These magnitude changes are negligible and no trends are noticed with a change in description to the total derivative matrix.

The next change studied was the starting inhibitor length due to its direct correlation to vortex shedding frequency and impact on Thrust Oscillation. To change the inhibitor length a 5% decrease in starting inhibitor length was made to the analysis which subsequently increases the starting vortex shedding frequency by roughly 5%. The analysis was ran and the A matrix for the analysis was captured and is shown below in Table 10.

Table 10. *A Matrix of Ares 1 with a 5% Decrease in Inhibitor Size*

	T/O	D_X	D_Y	A_1	A_2	A_3
T/O	1	9.2241	297.004	-459.9	-41.28	-17.64
D_X	85.0287	1	0	0	0	0
D_Y	458.928	0	1	0	0	0
A_1	0	-.3011	0	1	0	0
A_2	0	-.3011	0	0	1	0
A_3	0	-.3011	0	0	0	1

	Strong Coupling
	Moderate
	Weak Coupling

The sensitivity matrix captured with a decrease in inhibitor captures 2 major magnitude changes. The first is the decrease in magnitude in the displacement derivatives and their impact on T/O. This is consistent with the concept of transmissibility discussed earlier, where the loads of thrust oscillation are largest when the frequencies of the loads are coincidental to the acoustic resonance frequencies [22]. The second major magnitude change noticed is the change within the acoustic modes. As the vortex frequency changes and diverges from resonance, the minor changes in the acoustic resonance frequencies have a larger impact on T/O than previously found in Table 6. The total derivative matrix of a decrease in inhibitor length of 5% is shown below in Table 11.

Table 11. *Total Derivative Matrix of Ares 1 with a 5% Decrease in Inhibitor Size*

	L_I	U_f	P_C	A_C	A_E	E	L_C
T/O	-2.67E17	-1.0E12	160.73	6.17E13	-1.553E14	-1.1E-16	2.75E6
D_X	3.04E7	114.55	-1.83E-8	-7.04E3	1.77E4	0	-3.14E-4
D_Y	7.97E8	2.99E3	-4.8E-7	-1.84E5	4.63E6	0	-.0082
A_1	1.35E9	5.07E3	-8.125E-7	-3.12E5	7.85E6	0	-4.22
A_2	2.7E9	1.015E4	-1.625E-6	-6.24E5	1.57E6	0	-16.88
A_3	4.05E9	1.52E4	-2.437E-6	-9.36E5	2.35E6	0	-37.97

The total derivative matrix shows slight changes in magnitude, specifically the impacts that the design variables have on T/O. There seems to be a correlation to a larger impact the design variables have on T/O as the vortex shedding frequency approaches the first resonance mode. The region around the first resonance mode frequency seems highly nonlinear, as shown with the change in discretization size in Tables 8 and 9. This can be attributed to the transmissibility function that captures a larger magnitude of the pressure oscillation load on the inhibitor based on its proximity to resonance. A 4th analysis is proposed to test to see if similar impacts are noticed when the length of the inhibitor is increased by 5 % instead of decreased. Table 12 below shows the A matrix with an increase of the inhibitor length by 5%, which also implies an approximate increase of 5% in the vortex shedding frequency.

Table 12. *A Matrix of Ares 1 with a 5% Increase in Inhibitor Size*

	T/O	D_X	D_Y	A_1	A_2	A_3
T/O	1	17.9001	231.046	-385.2	-13.97	-9.01
D_X	84.8495	1	0	0	0	0
D_Y	457.865	0	1	0	0	0
A_1	0	-.6983	0	1	0	0
A_2	0	-.6983	0	0	1	0
A_3	0	-.6983	0	0	0	1

	Strong Coupling
	Moderate
	Weak Coupling

With an increase in inhibitor length of 5% a similar trend seems to appear, the impact that the displacement in the Y direction has on T/O decreases as the vortex shedding frequency gets further from the resonance mode. Its interesting to note that the magnitude derivative of displacement onto T/O in the X direction has increased. This could possibly be due to the fact that an increase in inhibitor length tends to block more flow, causing a greater pressure differential from before and after the inhibitor, which in turn has a greater load impact from the displacement in the X direction [27,28]. The total derivative matrix for the 5 % increase in inhibitor length analysis is shown below in Table 13.

Table 13. *Total Derivative Matrix of Ares 1 with a 5% Increase in Inhibitor Size*

	L_I	U_f	P_C	A_C	A_E	E	L_C
T/O	-4.99E17	3.29E13	470.22	1.735E14	-4.519E14	6.7E-17	2.91E6
D_X	8.648E7	-5.69E3	-8.141E-8	-3.0E4	7.825E4	0	-5.04E-4
D_Y	2.264E8	-1.49E5	-2.12E-6	-7.86E5	2.0472E6	0	-.0132
A_1	3.827E9	-2.522E5	-3.603E-6	-1.32E6	3.4637E6	0	-4.23
A_2	7.655E9	-5.045E5	-7.207E-6	-2.65E6	6.92E6	0	-16.9
A_3	1.14E10	-7.56E5	-1.081E-5	-3.98E6	1.039E7	0	-38.0

It's interesting to note that the total derivative matrix magnitudes don't change by much and are consistent with those found in the first analysis presented in Tables 6 and 7. The final analysis proposed is one where the starting vortex shedding frequency is far from the first acoustic mode of the engine. A trend was noticed where the impact onto T/O from the displacement of the inhibitor tended to decrease in magnitude as the starting vortex shedding frequency was further from resonance. To test this the inhibitor length was increased by 100%, or double its length, to test the impact this had on the coupling analysis. Below is Table 14 showcasing the local sensitivity matrix of the analysis where the inhibitor length was doubled.

Table 14. *A Matrix of Ares 1 with a 100% Increase in Inhibitor Size*

	T/O	D_X	D_Y	A_1	A_2	A_3
T/O	1	-.4662	-14.242	-365.2	-35.62	-22.26
D_X	85.0420	1	0	0	0	0
D_Y	459.007	0	1	0	0	0
A_1	0	-.2862	0	1	0	0
A_2	0	-.2862	0	0	1	0
A_3	0	-.2862	0	0	0	1

	Strong Coupling
	Moderate
	Weak Coupling

As the starting vortex shedding frequency moves further and further from the first acoustic mode the magnitude of the displacements impact on T/O continues to decrease as shown in the first row. The derivative in the X direction went from a moderate coupling when close to the resonance frequency to a weak coupling, where the derivative in the Y direction dropped substantially as well to a moderate coupling where before it was strong. This change is consistent with the correlations found earlier where the inhibitor displacement has a larger contribution to T/O depending on its starting length. Table 15 below showcases the total derivative matrix of the analysis.

Table 15. *Total Derivative Matrix of Ares 1 with a 100% Increase in Inhibitor Size*

	L_I	U_f	P_C	A_C	A_E	E	L_C
T/O	-1.03E17	7.61E14	-3.0057E3	-1.07E14	3.004E15	7.43E-17	8.13E6
D_X	1.145E7	-8.383E4	3.3107E-7	1.1803E5	-3.3094E5	0	-8.95E-4
D_Y	2.997E8	-2.19E6	8.663E-6	3.08E6	-8.6569E6	0	-.0234
A_1	5.073E8	-3.72E6	1.4663E-5	5.22E6	-1.4657E7	0	-4.25
A_2	1.014E9	-7.42E6	2.9325E-5	1.045E7	-2.9313E7	0	-16.9
A_3	1.521E9	-1.11E7	4.3988E-5	1.568E7	-4.397E7	0	-38.05

The total derivative matrix had slight changes in magnitude but no major trend was found from this analysis compared to the previous 4 analyses. The results are further discussed in the next section.

Results

Capturing the local coupling feedback from the displacement of the inhibitor back onto the magnitude of T/O would have given NASA insight to the unexpected event that occurred on the Ares 1 rocket. It was noticed within the analysis that the larger the deviation between the vortex shedding frequency and first acoustic mode, the smaller the coupling strength is. For cases where the deviation from the vortex shedding frequency and resonance frequency is large, the coupling might be suitable for suspension in a large optimization analysis. Elimination of the coupling however is not recommended as the coupling is extremely volatile to the vortex shedding frequency and can lead to large magnitudes of T/O if the coupling is not captured, as is shown in the cases where vortex shedding frequency is close to the resonance frequency. In each case it can be seen that the displacement in the length of the inhibitor is either a strong or moderate coupling and the feedback from structures back onto the fluids subsystem should have been monitored more closely by the engineers at NASA.

For future work an uncertainty analysis into the local and total derivative matrix can be made to determine these volatile derivatives and access a higher fidelity approach to the importance of the coupling on local subsystems. This is further discussed in the Conclusion Chapter of this research. The next Chapter titled Value Function goes over the creation of a value function for the purposes of testing the T/O's impact to mission success. The question of how important capturing the feedback interaction from the structures subsystem back onto the fluids subsystem will be evaluated in terms of a mission to the ISS. The value function will be formulated

and the elimination of the coupling analysis will be made to determine the magnitude of negative impact this feedback could have, if not captured, on mission success.

CHAPTER 6

ARES I VALUE FUNCTION

Value Function Formulation

The purpose of developing a value function and running a mission scenario with the Ares 1 is to test the impact that the T/O coupling has on the value of a system. Does capturing this feedback offer a greater mission success rate? If so, does the cost of modeling T/O prove to be a greater burden on the overall value of the system than simply eliminating the coupling? These questions will be accessed by developing a mission to the ISS using the design variables mentioned in Chapter 5. The design variables will be used to calculate the behavior variables that encapsulate the thrust needed to get to the ISS as well as the amount of payload that's carried. Then at an analysis of how elimination or perturbation of those couplings impact that total value of the system. To begin the formulation of the value function a breakdown of the mission profile is needed.

The mission to the ISS is broken down into two segments, the first being the first stage rocket motor that has been covered extensively in this research, and the second being the J-2X upper stage rocket engine. The mass and thrust of the J-2X will remain a constant, where the mass of the engine is 2470 kilograms and thrust is 1310 kilo newton's [39,43]. Once the total energy required to get to the ISS is calculated the amount of energy produced by the J-2X will be subtracted and the total energy needed for the first stage will be found. The mission profile that is then captured in the value function is simply the value produced by the first stage engine, the second stage engine is assumed to work and will offer no cost or benefit to the value function.

The method for finding the value associated with the first stage engine was to first identify the key design and behavior variables that have an impact on mission success. Once mission success is found, the cost associated with the mass of the structure and mass of the propellant is

found using the same design and behavior variables. This will put the terms of the value function in dollars and mission success rate. To capture the essence of mission success in terms of dollars the mission success rate will be a multiplicative term used to capture the revenue made from delivering the payload. In the case used for this analysis the average revenue derived from delivering 1 kilogram to the ISS is $22,000. The initial design and behavior variables that will be used to capture cost and mission success are provided below in Table 16.

Design Variables		Behavior Variables	
L_{it}	Length of Inhibitor	T/O	Thrust Oscillation Forcing Function
U_f	Velocity of Flow	ΔV	Energy from 1st Stage
R_C	Radius of Chamber	M_s	Mass of Structure
R_e	Radius at Exit	M_p	Mass of Propellant
P_C	Pressure of Chamber	A_1	First Acoustic Mode
L_C	Length of Chamber		

Table 16. *Design and Behavior Variables of the Value Function*

The value function is now captured in terms of profit, where the higher the mission success rate and lower the cost, the greater the profits achieved by the stakeholders. Profit is the true preference of the stakeholders and dollars is a unit that can universally be understood which gives the value function flexibility [40,44]. By using these metrics an analysis on how T/O impacts value can be made. The method to capture T/O in the value function is to use it both in the mission success rate and cost of the project. As analysis of T/O is captured the mission success rate of the Ares 1 will tend to grow, increasing profits. At the same time the more analysis done will also come at a cost, more engineering hours would be required to run the analysis and capture T/O.

To capture the impact T/O has on mission success rate the analysis done in Chapter 5 will be used. Depending on the design variables given, the magnitude of T/O can give varying levels

of vibrations, in some cases this can be detrimental to mission success, while in others it can have little to no impact. The analysis done in Chapter 4 to capture transmissibility is used to capture this relationship in T/O. As the vortex shedding frequencies tend toward the natural frequencies, the impact that T/O has on mission success is captured with the function shown in Figure 21 below.

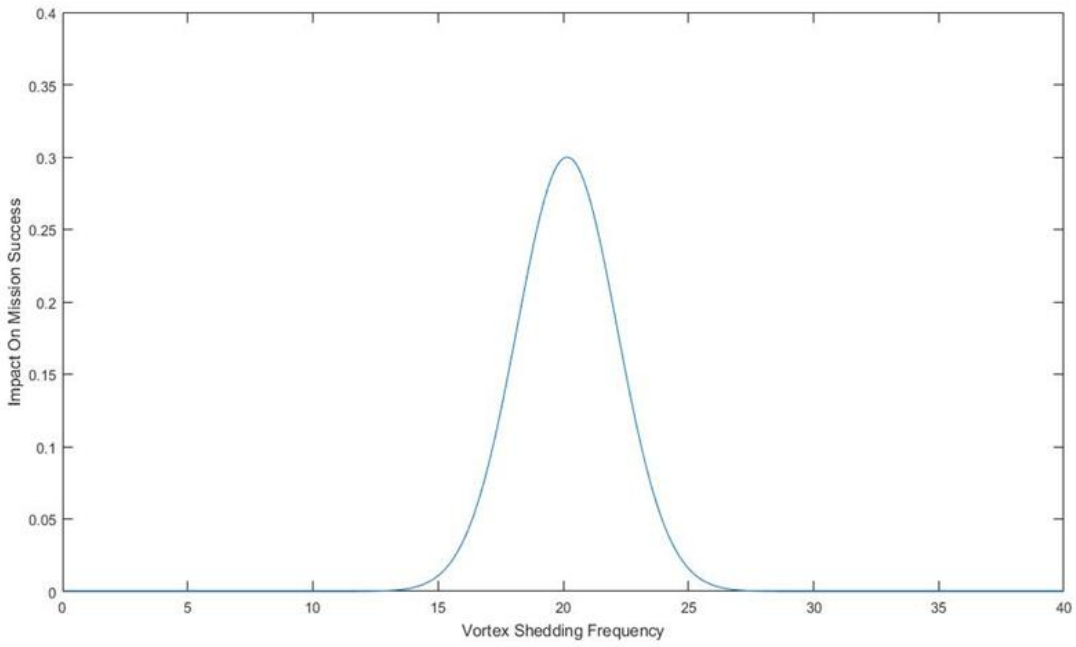

Figure 21. *Thrust Oscillations Impact on Mission Success*

Figure 21 was captured with an analysis where the starting design variables gave a resonance frequency of 20.1 Hz. It can be seen that as the vortex shedding frequency gets closer to resonance, the impact on mission success increases. A maximum negative impact of 30% to mission success was chosen for this analysis. The impact on mission success can vary depending on the rockets ability to dampen out the oscillatory forces produced by T/O, a safe estimate of 30% captures the true risk T/O can have on the off chance the engine hits the resonance frequency. Transmissibility was the key factor here, as the frequency gets further from resonance its impact to mission success degrades until little to no impact is noticed. Multiple analysis will be ran at varying impact levels to capture the value lost when eliminating the T/O coupling.

Once the physical impact that T/O has on value is captured a means of capturing the analysis time is made that affects the cost of the system. Engineering hours is used in this case to calculate the cost of running multiple simulations in order to mitigate T/O. The cost for one engineer to work 1 hour is set to be $100.00 an hour. For the first analysis a team of 100 engineers is chosen to attempt to mitigate T/O. For the case presented the engineering hours would therefore be $100.00 * 100 engineers, which is $10000.00 per engineering hour. If 2000 hours are put in by all engineers the mission success rate is positively impacted by 5 %, where the analysis time put in by the engineers represents the amount of analysis time spent on T/O. Typically this cost can vary depending on organization and amount of computation time required, which is why each value function is case specific [40]. These values for cost and mitigation success can be changed to accommodate better research into these subject, these values were simply chosen as a baseline to demonstrate the concept and value for capturing T/O. To evaluate the impact per hour that computation time has on the cost and impact on mission success rate the following function shown in Figure 22 is proposed.

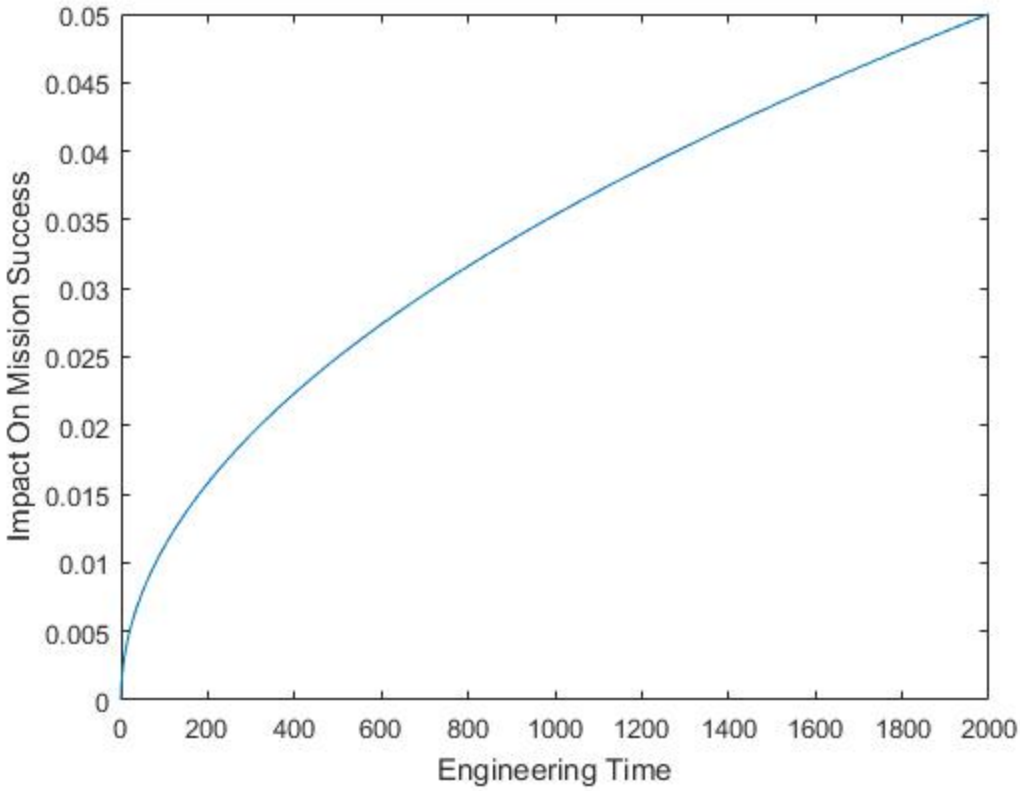

Figure 22. *Analysis Time vs Impact on Mission Success*

Here it can be seen that as more time is spent on the analysis the higher the impact on Mission Success is. The exponential nature of the function is aimed to represent the idea of diminishing returns which is prevalent in software development [41,42]. As more analysis time is spent the less impact each additional analyses hour has on the impact on mission success.

With the revenue and cost captured the value function can then be defined by the following equations:

$$System\ Value = Revenue - Cost \tag{29}$$

Where,

$$Revenue = Probability\ of\ Mission\ Sucess * Mass\ of\ Payload * \frac{Revenue}{Kg} \tag{30}$$

$$Cost = Mass\ of\ Propellant + Mass\ of\ Structure + Analysis\ Time \tag{31}$$

An analysis of the value function can now be ran to find the cost vs benefits of finding the T/O coupling information in terms of total profit. The analyses proposed will look at various scenarios that impact value that pertain to T/O. The first analysis will evaluate the impact that analysis time has on total value as it pertains to research time of T/O. The second analysis will look at different starting design variables, where the inhibitor will be looked at extensively, and evaluate the impact that T/O has on mission success. Once the general basis and understanding of the value function is known, a coupling suspension will be made and the impact on the value function will be determined with the methodologies discussed in Chapter 3 of this research paper.

Results

The first analysis of the value function will look at 10 different scenarios pertaining to the amount research time done on identifying the T/O coupling. Initial conditions set for the design variables are that of the Ares 1, with a normalization factor to protect ITAR data. Each scenario will capture the total profit earned vs the amount of research done. Table 17 below showcases the first analysis.

Table 17. *Research Time vs Profit*

Analysis Time on T/O	Value in terms of Dollars
0 Hours	$ 26,164,371
200 Hours	$ 33,155,612
400 Hours	$ 34,879,906
600 Hours	$ 35,737,657
800 Hours	$ 36,146,853
1000 Hours	$ 36,269,397
1200 Hours	$ 36,188,323
1400 Hours	$ 35,952,958
1600 Hours	$ 35,595,441
1800 Hours	$ 35,138,094
2000 Hours	$ 34,597,171

With the initial conditions and functions describing T/O set, a comparative analysis shows that analysis time has a greater benefit in terms of value then simply ignoring the possibility of having T/O occur. Their is a value loss associated with more analysis time after 1000 hours. This is because the value captured by the impact of mission success is less than the associated cost of running the analysis. It can then be shown the value of capturing the feedback of T/O from structures back to fluids is greater than the cost it would take to run the analysis. The second analysis shown in Table 18 looks at 10 different inhibitor sizes and its impact to the value of the system. The analysis time of the workers in this scenario is set to 0.

Table 18. *Inhibitor Length vs Profit*

Inhibitor Length	Value in terms of Dollars
.090 Meters	$ 92,512,393
.095 Meters	$ 34,713,943
.100 Meters	$ -15,254,053
.105 Meters	$ -29,272,409
.110 Meters	$ -7,238,846
.115 Meters	$ 26,164,371
.120 Meters	$ 70,169,328
.125 Meters	$ 99,064,104
.13 Meters	$ 117,766,942
.135 Meters	$ 128,698,593
.14 Meters	$ 134,657,304

The value of the system is heavily dependent on mitigating the occurrence of T/O and its magnitude. When vortex shedding is within the resonance frequency of the engine the value of the system is negative, meaning the costs of operation of the Ares 1 outweighs the revenue produced from the payload. These drastic changes occur due to the high impact value that T/O has on the system, where when T/O hits resonance an impact of 30% to mission success is noticed. As the inhibitor length gets larger or shorter the vortex shedding frequency gets further from resonance and therefore increasing the rate of mission success and capturing more profit.

Now that the value function is formulated and changes in behaviors captured a coupling suspension can be made where the impacts to the overall all value function are recorded. The methodology for this analysis is discussed extensively in Chapter 3 of this research. By taking Eq. 14 the total change in value can be found from the suspension of one coupling. Table 19 below shows the results of perturbing each coupling by 5% and noting the changes in total value.

Table 19. *Change in Value due to Coupling Perturbation*

Coupling Perturbed	Change in Value
$\frac{TO}{D_x}$	$ 33,749.87
$\frac{TO}{D_y}$	$ 171,382.44
$\frac{TO}{A_1}$	$ 124,850.52
$\frac{TO}{A_2}$	$ 49,809.30
$\frac{TO}{A_3}$	$ 2,886.57
$\frac{D_x}{TO}$	$ 495,135.65
$\frac{D_y}{TO}$	$ 550,911.54
$\frac{A_1}{D_x}$	$ 0
$\frac{A_2}{D_x}$	$ 0
$\frac{A_3}{D_x}$	$ 0

It is noticed from a comparative analysis that the behavior variable T.O. has the greatest impact on the change in value when it is perturbed by 5% shown by Dx/TO and Dy/TO The impact onto the value caused by the feedback from the subsystem structures back onto the fluids subsystem is shown by TO/Dx and TO/Dy. A value change of $171,382.44 is noticed by the displacement in the Y direction, showcasing a high impact on value. If running an analysis it would be within the best interest of the stakeholders to consider keeping this coupling, and in the case of NASA, further evaluation of the feedback structures has on the fluid flow within the engine.

The value function presented here offers a potential means of capturing the T/O's impact to the overall profit of the mission. It can be seen that there is a return on investment into running a local coupling analysis, where the more time invested gathered higher profits for the

stakeholders. The earlier this is done during the design and development phase of any LSCES the higher the likelihood of capturing these unexpected behaviors and mitigating them with little additional costs. Capturing the change in value due to perturbations in the sensitivity matrix gives engineers and managers a good overview of the systems that have high impact on value. This insight could have aided the team at NASA to consider further investigation into the feedback from structures to fluids that was considered a small contribution to T/O during the design and development phase. Future work can be made into the impact that mission failure can have on potential funding of NASA. A congressional model is proposed as a possible means to capture public perception of NASA and its missions, where greater funding can be related to the general public's approval of NASA and its missions. Further details of this model will be discussed in the conclusions section of this research.

CHAPTER 7

CONCLUSION

Summary and Conclusion

This research project takes the concepts of a coupling strength analysis from MDO and applies it to a real event that occurred in a LSCES. A forensics study into the design and development phase of the Ares 1 was made in order to determine if a coupling strength analysis would have identified the issue of T/O. The coupling strength analysis looked at feedbacks and feed forwards of behavior variables that aren't normally captured when the analysis of T/O is broken down by disciplines and done separately with no iterative process to capture changes. Through the breakdown of 3 major disciplines, it was shown that the inhibitors displacements within the rocket engine was a moderate to strong coupling that should have been captured within the analysis and not deemed inconsequential by NASA. This research paper is an advocate of using these methods in order to determine unexpected behaviors that may arise during the operation of LSCES.

To test the impact that the elimination of this coupling had on mission success a value function was developed from the field of VDD. With a value perspective frame of mind, it was noticed that the benefits of running a multidisciplinary coupling analysis outweighed the costs. Both mission success rate of the engine and profit derived from the impact increased, with more analysis time aiding to larger profits for shareholders. The value function method presented within this research is flexible and can be modified for other various missions. The impact that the analysis and mission success rate have on value can be changed and further developed with more research. To tie the value function with the coupling analysis a suspension of each coupling was made to evaluate the change in value associated with a 5 % perturbation. It was noticed that the

feedback had a larger impact on total value than previously captured, giving more merit to developing a coupling analysis to capturing unexpected consequences in LSCES.

Future Work

Further research into an uncertainty model is proposed to capture the variability of couplings within a sensitivity matrix. It was noticed during analysis that the displacement coupling had high variability depending on the discretization size used. An uncertainty model can capture this variability and give greater insight to engineers and managers to the potential magnitude of these specific couplings. Further research can then be made in determining the probability of the maximum magnitude to occur within the sensitivity analysis.

Another proposed research topic is a higher fidelity value function that captures congressional support. The impact of a successful mission of the Ares 1 doesn't just capture the benefits of the payload reaching orbit, rather it encourages trust in NASA and possible future missions. A congressional value model is proposed as a means to capture the public's perception of NASA missions and aim to determine the impact of a mission failure can have not only from the cost of the payload but also the public's backlash that could possibly reduce further missions.

REFERENCES

1. Hajela, P., Christina L. Bloebaum, and Jaroslaw Sobieszczanski-Sobieski. "Application of global sensitivity equations in multidisciplinary aircraft synthesis." Journal of Aircraft 27.12 (1990): 1002-1010.
2. Constellation program: Ares I-X flight test vehicle. Retrieved from https://www.nasa.gov/pdf/354470main_aresIX_fs_may09.pdf
3. Zhang Q, Wei Z, Su W, Li J, Wang N. Theoretical modeling and numerical study for thrust-oscillation characteristics in solid rocket motors. Journal of Propulsion and Power 2012; 28:2. p. 312-322
4. Culick FEC. Combustion instabilities in solid propellant rocket motors. Internal Aerodynamics in Solid Rocket Propulsion, Belgium. 2002.
5. Constellation. Constellation finalizes thrust oscillation fix. 21 December 2009. Retrievedfrom https://blogs.nasa.gov/Constellation/2009/12/21/post_1261434125038/
6. Bloebaum, Christina L., and A. R. McGowan. "The design of large-scale complex engineered systems: present challenges and future promise." Proceedings of the 14th AIAA/ISSMO Multidisciplinary Analysis and Optimization Conference, Indianapolis, IN, Paper No. AIAA-2012-5571. 2012.
7. NASA, NASA Systems Engineering Handbook. Vol. NASA/SP-2007- 6105 Rev1. 2007, Washington, D.C.
8. Forsberg, Kevin, and Harold Mooz. "7.17. System Engineering for Faster, Cheaper, Better." INCOSE International Symposium. Vol. 8. No. 1. 1998.
9. Collopy, Paul. "Economic-based distributed optimal design." AIAA Space 2001 Conference and Exposition. 2001.
10. Castagne, Sylvie, et al. "Value driven design optimization of aircraft structures." 6th AIAA Aviation Technology, Integration and Operations Conference (ATIO). 2006.
11. Buede, D.M., The Engineering Design of Systems : Models and Methods. Vol. 55. 2009: John Wiley & Sons
12. Martins, Joaquim RRA, and Andrew B. Lambe. "Multidisciplinary design optimization: a survey of architectures." AIAA journal 51.9 (2013): 2049-2075.
13. English KW. Development of multiple cycle coupling suspension in multidisciplinary design optimization. M.S Thesis. State University of New York at Buffalo 1998.
14. Sobieszczanski-Sobieski, Jaroslaw. "A linear decomposition method for large optimization problems. Blueprint for development." (1982).
15. Bloebaum, Christina L., Prabhat Hajela, and Jaroslaw Sobieszczanski-Sobieski. "Non-hierarchic system decomposition in structural optimization." Engineering Optimization+ A35 19.3 (1992): 171-186.
16. Sobieszczanski-Sobieski, J., Sensitivity of complex, internally coupled systems. AIAA journal, 1990. 28(1): p. 153-160.
17. Bloebaum, C., and J. Sobieszczanski-Sobieski. "Sensitivity based coupling strengths in complex engineering systems." 34th Structures, Structural Dynamics and Materials Conference. 1993.
18. Souto, Carlos d'Andrade. "Liquid rocket combustion chamber acoustic characterization." Journal of Aerospace Technology and Management 2.3 (2010): 269-278.
19. Yang, Vigor, Joseph M. Wicker, and Myong W. Yoon. "Acoustic waves in combustion chambers." Liquid rocket engine combustion instability(A 96-11301 01-20), Washington,

DC, American Institute of Aeronautics and Astronautics, Inc.(Progress in Astronautics and Aeronautics. 169 (1995): 357-376.
20. Laudien, E., et al. "Experimental procedures aiding the design of acoustic cavities." Progress in Astronautics and Aeronautics 169 (1995): 377-402.
21. Young, H.D.; and Freedman, R.A.; Ford, A.L. (contributing author). 2012. Sears and Zemansky's University Physics with Modern Physics. 13th ed.Pearson Education, Inc., Addison-Wesley, San Francisco, CA, USA
22. D. J. Inman. "Engineering Vibration", 3rd Edition. Upper Saddle River, NJ, 2008, Pearson Education, IncThrust
23. Culick, F. E. C., and K. Magiawala. "Excitation of acoustic modes in a chamber by vortex shedding." Journal of Sound and Vibration 64.3 (1979): 455-457.
24. CD-adapco. STAR-CCM+ 9.06.009 [computer software]. New York, Melville 2014
25. Doston, KW, Koshigoe A. Vortex shedding in a large solid rocket motor without inhibitors at the segment interfaces. Journal of Propulsion and Power 1997; 13:2. p. 197-206.
26. Kenny RJ, Hulka J, Jones G. Cold flow testing for liquid propellant rocket injector scaling and throttling. 42nd AIAA/ASME/SAE/ASEE Joint Propulsion Conference, Sacramento, 2006.
27. Hunt, Julian CR, Alan A. Wray, and Parviz Moin. "Eddies, streams, and convergence zones in turbulent flows." (1988).
28. Moffatt, H. K. "Viscous and resistive eddies near a sharp corner." Journal of Fluid Mechanics 18.01 (1964): 1-18.
29. Knisely, Charles W. "Strouhal numbers of rectangular cylinders at incidence: a review and new data." Journal of Fluids and Structures 4.4 (1990): 371-393.
30. Mason, Donald, et al. "Pressure oscillations and structural vibrations in space shuttle RSRM and ETM-3 motors." 40th AIAA/ASME/SAE/ASEE Joint Propulsion Conference and Exhibit. 2004.
31. ANSYS Inc. ANSYS 15.0 [computer software] Pennsylvania, Canonsburg 2013
32. Dotson, K. W., S. Koshigoe, and K. K. Pace. "Vortex shedding in a large solid rocket motor without inhibitors at the segment interfaces." *Journal of Propulsion and Power* 13.2 (1997): 197-206.
33. Chapline, Gail. *Journal of Materials and Manufacturing*. Warrendale, PA: SAE International, 2006. Web
34. Guery, J., et al. "Thrust oscillations in solid rocket motors." *44th AIAA/ASME/SAE/ASEE Joint Propulsion Conference & Exhibit*. 2008.
35. Blomshield, Fred. "Lessons learned in solid rocket combustion instability." *43rd AIAA/ASME/SAE/ASEE Joint Propulsion Conference & Exhibit*. 2007.
36. Zill, Dennis G. *A First Course In Differential Equations.* 5th ed. Pacific Grove, Calif: Brooks/Cole, 2001. Print.
37. Ballereau, Severine, et al. "Evaluation method of thrust oscillations in large SRM-application to segmented SRM's." *47th AIAA/ASME/SAE/ASEE Joint Propulsion Conference & Exhibit*. 2011.
38. Davenas, Alain, ed. *Solid rocket propulsion technology*. Newnes, 2012.
39. Mark Wade (17 November 2011). "J-2X". Encyclopedia Astronautica.
40. Hazelrigg, George A. "A framework for decision-based engineering design." *Transactions-American Society of Mechanical Engineers Journal of Mechanical Design* 120 (1998): 653-658.

41. Boehm, Barry. "Value-based software engineering: reinventing." *ACM SIGSOFT Software Engineering Notes* 28.2 (2003): 3.
42. Boehm, Barry W. *Software engineering economics*. Vol. 197. Englewood Cliffs (NJ): Prentice-hall, 1981.
43. Mesmer, Bryan L., C. L. Bloebaum, and H. Kannan. "Incorporation of value-driven design in multidisciplinary design optimization." *10th World Congress on Structural and Multidisciplinary Optimization*. 2013.
44. Collopy, Paul D., and Peter M. Hollingsworth. "Value-driven design." *Journal of Aircraft* 48.3 (2011): 749-759.
45. Rogers, J. A. M. E. S., and Christina Bloebaum. "Ordering design tasks based on coupling strengths." *5th Symposium on Multidisciplinary Analysis and Optimization*. 1994.
46. ATK Space Systems, Janssen, J. *Pressure/Thrust Oscillation Forcing Functions for the SLS Booster*. EM001407 Rev. B.
47. ATK Space Systems, Janssen, J. *Pressure/Thrust Oscillation Transient Forcing Functions for the SLS Booster Motor*. TR027646 Rev. C.
48. ATK Space Systems, Kofford, A. Milano, D. *Ares 1 Dynamic Pressure to Force Conversion*. TR022382 Rev. A.
49. Collopy, Paul. "Aerospace system value models: A survey and observations." *AIAA Space 2009 Conference & Exposition*. 2009.
50. Sobieszczanski-Sobieski, Jaroslaw, and Raphael T. Haftka. "Multidisciplinary aerospace design optimization: survey of recent developments." *Structural optimization* 14.1 (1997): 1-23.
51. Bloebaum, C. L. "Coupling strength-based system reduction for complex engineering design." *Structural and Multidisciplinary Optimization* 10.2 (1995): 113-121.
52. BLOEBAUM, CHRISTINA. "Global sensitivity analysis in control-augmented structural synthesis." *27th Aerospace Sciences Meeting*. 1989.
53. Sobieszczanski-Sobieski, Jaroslaw, Christina L. Bloebaum, and Prabhat Hajela. "Sensitivity of control-augmented structure obtained by a system decomposition method." *AIAA journal* 29.2 (1991): 264-270.